

**A STUDY OF THE PRESSURE-INDUCED FUNDAMENTAL
ROTATION-VIBRATION BAND OF DEUTERIUM
IN DEUTERIUM-FOREIGN GAS MIXTURES
AT ROOM TEMPERATURE**

CENTRE FOR NEWFOUNDLAND STUDIES

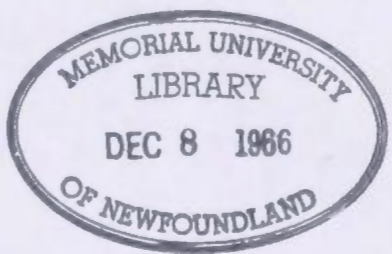
**TOTAL OF 10 PAGES ONLY
MAY BE XEROXED**

(Without Author's Permission)

SIU TING PAI

15651

21





**A STUDY OF THE PRESSURE-INDUCED FUNDAMENTAL
ROTATION-VIBRATION BAND OF
DEUTERIUM IN DEUTERIUM-FOREIGN GAS MIXTURES AT ROOM TEMPERATURE**

by



Siu Ting Pai, B.Sc.

**Submitted in partial fulfilment
of the requirements for the degree of Master of Science
Memorial University of Newfoundland**

September, 1965

This thesis has been examined and approved by:

D. H. Rendell, M.Sc., Ph.D.

**Assistant Professor of Physics
Memorial University of Newfoundland**

J. L. Hunt, B.A., M.A., Ph.D.

**Associate Professor of Physics
University of Guelph**

ABSTRACT

The pressure-induced fundamental infrared absorption band of deuterium has been studied in D_2 -He, D_2 -A and D_2 - N_2 mixtures for a series of pressures up to 1200 atm at room temperature. The absorption profile of each mixture shows a well-resolved splitting of the Q branch into two components, Q_P and Q_R , whose separation was found to increase linearly with the total density of the mixture. The contours of D_2 -A and D_2 - N_2 mixtures also show fairly well resolved S(2) peak and indications of several other S and O peaks of the band, while these are absent in the contours of D_2 -He mixtures. Using the theory and the observed line shape, an attempt was made to decompose the observed contours of D_2 -A and D_2 - N_2 mixtures. The overlap parts of the Q branches for D_2 -A and D_2 - N_2 mixtures thus obtained were studied together with the observed contours for D_2 -He mixtures which were found to consist mainly of the overlap part of the Q branch.

The integrated absorption coefficient of the band in the mixtures was found to follow an empirical power series in terms of the partial densities of the component gases. From this series the binary and ternary absorption coefficients were determined for each binary mixture. The theory proposed by Van Kranendonk was applied to the coefficient of the individual lines of the O and S branches as well as the quadrupole and overlap parts of the Q branch.

TABLE OF CONTENTS

CHAPTER		Page
I	INTRODUCTION	1
	The Fundamental Band of Hydrogen and Deuterium .	1
	Other Infrared Absorptions of Hydrogen	5
II	EXPERIMENTAL	8
	Gas Absorption Cell	8
	Optical Arrangement	10
	Experimental Procedure	12
III	RESULTS AND DISCUSSION	16
	Absorption Profile	16
	The Absorption Coefficients	23
IV	THEORY AND CALCULATION	32
	The Theory of Binary Absorption Coefficient in Mixtures	34
	Calculation for the Deuterium-Foreign Gas Mixtures	38

CHAPTER	Page
V CONTOUR ANALYSIS	44
The Absorption Profile of D ₂ -He Mixture	45
The Absorption Profiles of D ₂ -A and D ₂ -N ₂ Mixtures	53
ACKNOWLEDGMENT	62
APPENDIX	63
REFERENCES	67

CHAPTER I
INTRODUCTION

The Fundamental Band of Hydrogen and Deuterium

Since the fundamental absorption band of hydrogen induced by intermolecular forces was first observed by Welsh, Crawford and Locke (1949), the band has been studied very extensively under a variety of experimental conditions. It was investigated in pure hydrogen as well as in hydrogen-foreign gas mixtures by Chisholm and Welsh (1954) at pressures up to 1,500 atm at temperatures in the range of 78°K to 376°K, and later by Hare and Welsh (1958) at pressures up to 5,000 atm at room temperature. These authors have made detailed studies of the splitting of the Q branch, and also determined the binary and ternary absorption coefficients of the band. The splitting of the Q branch was interpreted by the above authors as due to the interaction of the relative kinetic energies of the colliding molecules in the process of absorption. Recently the studies of the band in the pure gas and in hydrogen-helium mixtures at temperatures in the range of 18°K to 77°K by Watanabe and Welsh (1964, 1965) lead to the discovery of bound states of $(H_2)_2$ complex.

The fundamental band of hydrogen has also been studied in liquid and solid states with various ortho-para ratios by various authors (Allin, Hare and Welsh 1955; Hare, Allin and Welsh 1955; Gush, Hare, Allin and Welsh 1960), and for hydrogen dissolved in liquid argon by Ewing and Trajman (1964). In these studies at low temperature, the absorption band

exhibited well-resolved rotational structure, and additional information concerning the nature of the Q components as well as the rotational structures of the band were obtained.

Although deuterium is an isotope of hydrogen, the induced infrared absorption band of deuterium has not been studied as extensively as that of hydrogen. A preliminary study of the induced fundamental absorption band of deuterium in pure deuterium and in deuterium-foreign gas mixtures was first made by Chisholm (1952). A detailed study of the band in pure deuterium was made later by Reddy and Cho (1965), and the absorption coefficients of pure deuterium have been determined. However, detailed studies of the induced fundamental band of deuterium in deuterium-foreign gas mixtures have not been made before the present investigation. However some studies on this band of deuterium in gaseous phase at low temperatures (Watanabe and Welsh 1965), as well as in liquid and solid states (Allin, Gush, Hare, Hunt and Welsh 1959) have been made. Watanabe and Welsh have shown that the bound states of $(D_2)_2$ complex exist in gaseous deuterium at low temperature.

The general appearance of the fundamental band of deuterium at room temperature has been observed to differ somewhat from that of hydrogen. In order to illustrate the difference, a schematic diagram of the rotational energy levels for the fundamental vibration absorption band of deuterium is presented in Fig. 1. In this figure the possible rotational transitions for the induced fundamental absorption band of

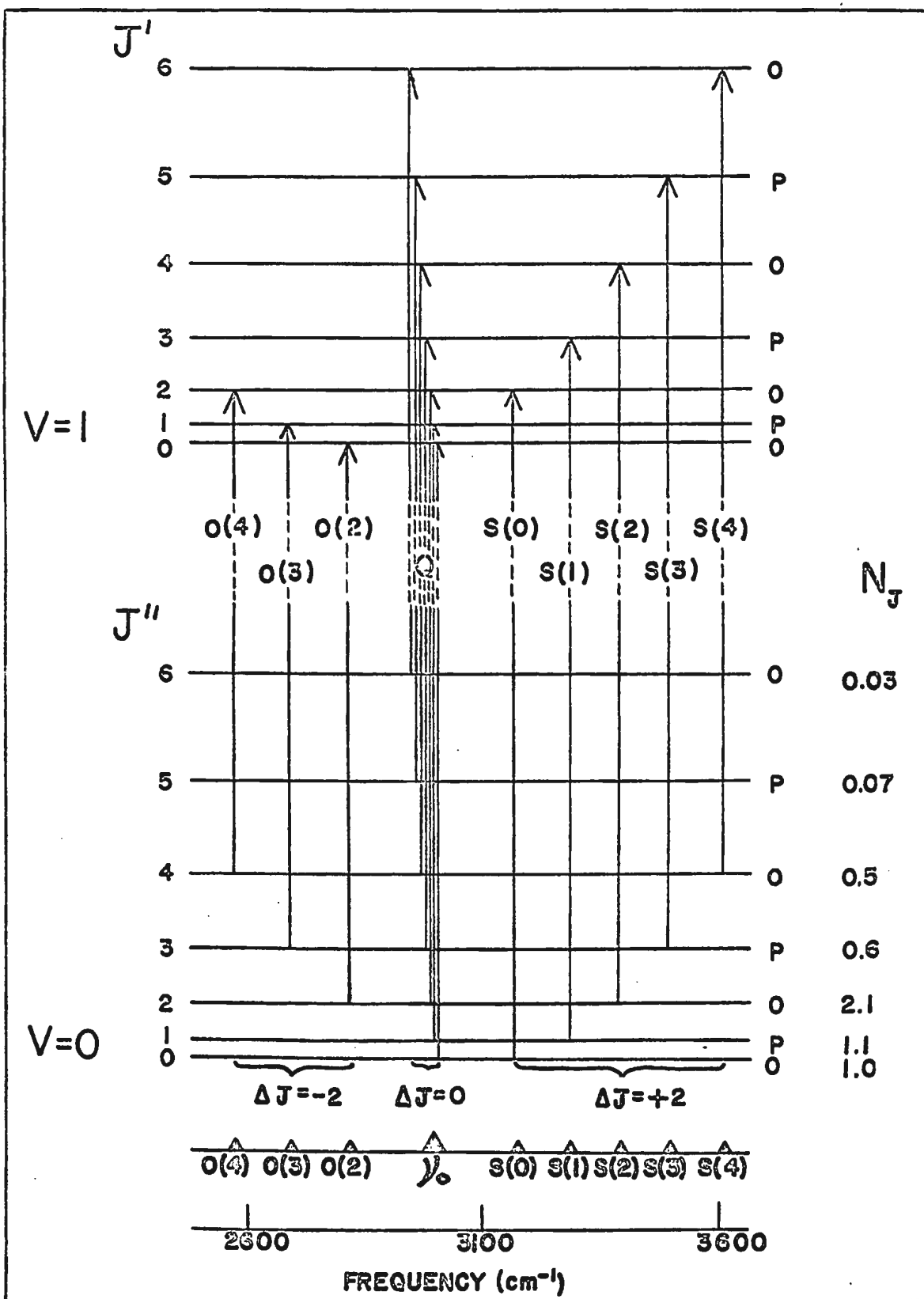


Fig. 1 Energy level diagram of the induced fundamental band of deuterium.

deuterium are indicated by vertical lines with arrow-head, and the approximate positions of the rotational lines, calculated from the molecular constants of the free molecule determined from the Raman spectrum of gaseous deuterium (Stoicheff 1957), are marked under the corresponding transitions. These transitions follow the selection rule for induced absorption of homonuclear diatomic molecules, $\Delta J = 0, \pm 2$, giving rise to the Q, S and O branches respectively, which is the same as in the case of Raman Spectra. Here J is the rotational quantum number. The relative population of the molecules at room temperature in each rotational energy level, as calculated from the Boltzmann distribution law and the statistical weights of the level, arising from the $(2J + 1)$ -fold degeneracy and the nuclear spin, is also shown in Fig. 1. Since the rotational constant of hydrogen molecule is roughly twice as large as that of deuterium molecule, it can be expected that the rotational levels of the lowest vibrational state of deuterium have higher relative population than the corresponding levels of hydrogen at the same temperature. Moreover the nuclear spin angular momentum of deuterium atom is $h/2\pi$, giving the statistical weight ratio of 6:3 for the states of the even and odd J values respectively; whereas for the case of hydrogen the nuclear spin angular momentum is $h/4\pi$ which gives the ratio 1:3 for the states of the even and odd J values respectively. Because of the above properties of deuterium molecules one may expect larger number of rotational lines in each branch of the fundamental band of deuterium than that of the

fundamental band of hydrogen. This fact may introduce additional complication for the analysis of the absorption contours of deuterium obtained at room temperature. In Fig. I, each rotational energy level was designated as O and P to indicate ortho and para modifications respectively.

Other Infrared Absorptions of Hydrogen

The induced first overtone band of hydrogen was investigated by Welsh, Crawford, MacDonald and Chisholm (1951), and later by Hare and Welsh (1958). The pure rotational spectrum of hydrogen was observed for the first time by Ketelaar, Copla and Hooge (1955). A more detailed study was made by Copla and Ketelaar (1958), Kiss, Gush and Welsh (1959) and Kiss and Welsh (1959). The latter authors found that the rotational spectrum appeared to be superimposed on a continuum which was postulated to arise from pure translational absorption. These authors obtained the absorption coefficients of the band, and made a detailed analysis of the shape of rotational lines. They found that an individual line in the pure rotational spectrum of hydrogen at 80°K could be well represented by a dispersion line shape for the high frequency wing of the line and by a dispersion line shape modified by the Boltzmann factor for its low frequency wing. By assuming a similar shape for the lines, Hunt and Welsh (1964) made an analysis of the absorption profiles of induced fundamental band of hydrogen.

Theory

The theory of the induced fundamental band of homonuclear diatomic molecules has been given by Van Kranendonk and Bird (1951), Van Kranendonk

(1957, 1958), and Britton and Crawford (1958). They have shown that, in particular reference to the induced fundamental band of hydrogen in pure gas and in hydrogen-foreign gas mixtures, the absorption due to binary collisions can be explained in terms of the electron overlap interaction and the molecular quadrupole interaction. In the first interaction, the induced electric dipole moment decreases exponentially with the intermolecular distance R , while in the second interaction, the induced electrical dipole moment varies as R^{-4} . According to the so-called "exp-4" model, the electric dipole moment induced by the short-range overlap forces is, in the first-order approximation, spherically symmetric, i.e. only slightly dependent on the relative orientation of the molecules in a colliding pair, and produces mainly transitions for which $\Delta J = 0$, i.e. the Q branch. The long-range quadrupole interaction, on the other hand, is strongly dependent on the mutual orientation of the colliding pair, and produces transitions for which $\Delta J = \pm 2$, i.e. S and O branch, and in addition, some contribution to the Q-branch intensity. The above theory developed by Van Kranendonk has been applied to the experimental results obtained in the studies of hydrogen band, and recently in the study of deuterium band in pure gas (Reddy and Cho 1965). It was found that the theory was sufficiently accurate for the explanation of the experimental results. The theory has also been modified for the pure rotational band of hydrogen by Van Kranendonk and Kiss (1959).

In the present investigation, the fundamental absorption band of deuterium was studied in deuterium-helium, deuterium-argon and deuterium-nitrogen mixtures at pressures up to 1,200 atm, at room temperature. The purpose of the present study is to determine the binary and ternary absorption coefficients and to make a comprehensive study of the absorption contours in various mixtures. The theory concerning the binary absorption coefficients proposed by Van Kranendonk was applied to the experimental results obtained in the present investigation and the necessary calculations were made.

CHAPTER II

EXPERIMENTAL

Gas Absorption Cell

The transmission type absorption cell used in the present investigation at pressures up to 1,200 atm is shown in Fig. 2. It has been previously described by Snook (1962) and Stevenson (1965). It consists mainly of the cell body, A, which was constructed of stainless steel $3\frac{1}{2}$ in. in diameter with a core of $\frac{3}{4}$ in. A stainless steel light guide, G, made of two sections, having a central bore of rectangular cross-section $\frac{13}{16}$ in. x $1\frac{1}{12}$ in. was inserted into the bore of the cell body. The inside surface of the light guide was polished to assure good reflection of light. Both the entrance and exit windows, W, were polished synthetic sapphire plates, 1 in. in diameter and 10 mm thick. They were cemented on to stainless steel window plates, B, by means of the General Electric Glyptol. The surface of the window plates, on which the window was cemented, was polished optically flat to ensure a good pressure seal. The windows were secured by steel caps, C, with Teflon washers, D, so that the cell could be evacuated without the windows becoming loose. The apertures in the window plates were rectangular having dimensions $\frac{3}{8}$ in. x $\frac{3}{16}$ in.

The absorption cell was held "pressure tight" by means of heavy steel closing nuts, E, with Teflon washers, F, placed between the window plates and the main cell body. The portion, B₁, of the window plates, with a thickness of $\frac{3}{8}$ in. was square in shape and fitted into a matched

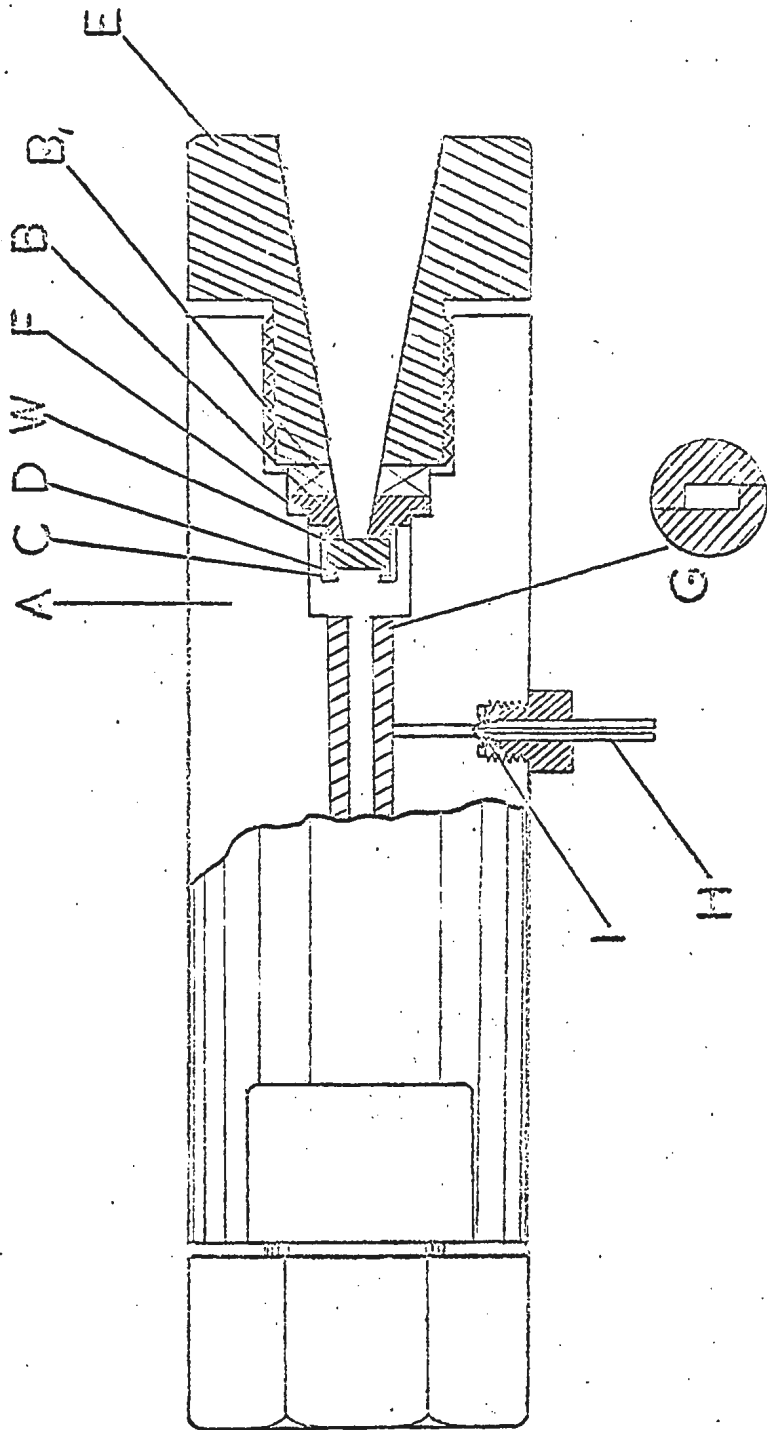


Fig. 2. High Pressure Gas Absorption Cell.

recess in the cell body, so that it could prevent non-alignment of the light guide and the window plat apertures when the nut was tightened. A 1/4 in. diameter steel capillary tube, H, served as the gas inlet to the cell and was connected by means of an Aminco fitting, I. The effective length of the cell was 11.4 cm.

Optical Arrangement

The optical system used with the transmission cell is shown schematically in Fig. 3. Infrared radiation from the source, S, was focused on the entrance window of the cell, H, by means of an aluminized spherical front surface mirror, M_1 . The radiation from the exit window of the cell was then focused onto the slit, S_1 , of the spectrometer, A, by means of a second spherical mirror, M_2 . In order to match the internal optics of the spectrometer, an F/4 light cone was used throughout the external arrangement.

A Perkin-Elmer 12C spectrometer with LiF prism and an Unicam Pneumatic Golay detector (G in Fig. 3) were used to measure the spectra in the present investigation. A water-cooled globar operated at a power of about 100 Watts from a Sorenson voltage regulator, was used as the source of the infrared continuum. The slit width of the spectrometer was maintained at 200 μ which gave a spectral resolution of approximately 11 cm^{-1} at 2993 cm^{-1} , the origin of the fundamental band of deuterium. The spectrometer was calibrated for the region 2,400 cm^{-1} - 3,800 cm^{-1} using water band and liquid indene bands of known frequencies. (Thomson, I.U.P. A.C. 1961). In reducing the recorder traces of the absorption

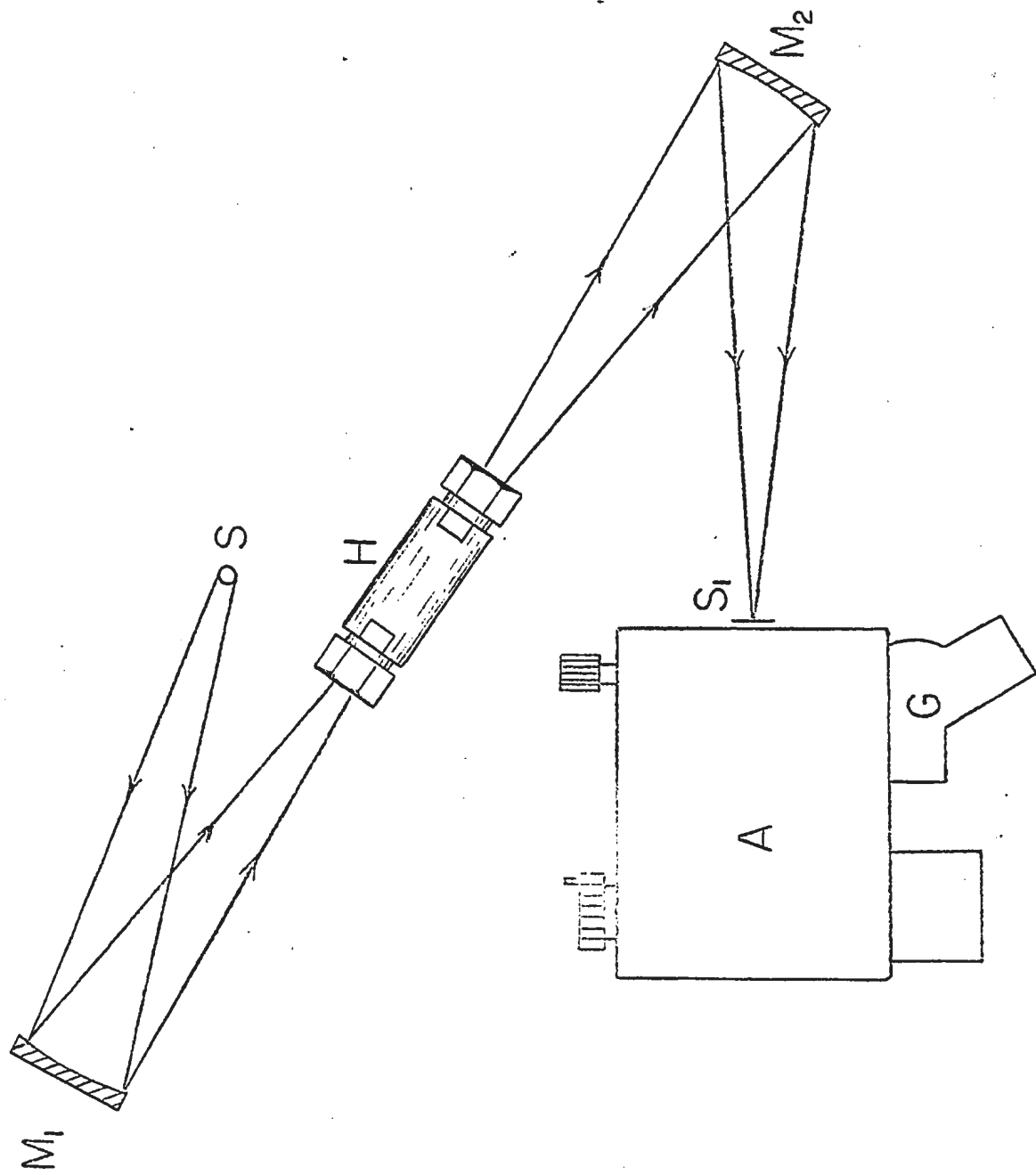


FIG. 3 Optical arrangement.

contours, the water band at $3,700 \text{ cm}^{-1}$ which appeared on each trace was used as a frequency reference.

For the purpose of analysis of the results obtained in the present investigation, it was required to study the foreign gas-enhanced absorption alone for each deuterium-foreign gas mixture. The pure "enhancement" absorption contour for each mixture, without the contribution from the absorption due to "pure deuterium", was constructed as follows: With the experimental procedure described below, the recorder trace of the absorption arising due only to the deuterium gas in a given mixture was made available. Comparing such "pure deuterium" absorption with the absorption due to the mixture, the quantity $\log_{10}(I_1/I_2)$ was obtained at a given frequency. Here I_1 is the signal transmitted by the cell filled with the component deuterium gas only and I_2 is the signal with the mixture in the cell. The enhancement absorption contour at each deuterium-foreign gas mixture was obtained by plotting the quantity $\log_{10}(I_1/I_2)$ against the frequency in cm^{-1} at intervals of 10 cm^{-1} across the band. The enhancement absorption coefficient $\alpha(\nu)$ may be defined as $(1/\ell)\log_e(I_1/I_2)$, where ℓ is the effective length of the absorption cell. The integrated absorption coefficient for the enhancement, $\left(\int \alpha(\nu) d\nu\right)_{\text{enhancement}}$ in cm^{-1}/cm was determined by measuring the area between the absorption contour and the frequency axis, and multiplying it by $(1/\ell)\log_e 10$.

Experimental Procedure

Prior to each experiment for deuterium-helium, deuterium-argon and deuterium-nitrogen mixtures, the entire system was evacuated to a pressure of 0.1 mm Hg for several hours. A series of recorder traces was taken with the absorption cell evacuated until a good reproduction of the background spectrum was obtained.

The gases used in the present investigation were introduced into the absorption cell by the system whose schematic diagram is shown in Fig. 4. For each mixture experiment, deuterium gas at a given pressure was first introduced from a commercial cylinder, supplied by Matheson of Canada Ltd., into the cell, C, through two liquid nitrogen traps, A. Absorption spectrum of the pure deuterium gas was then recorded. After the part between the needle valves V_2 and V_5 was re-evacuated, with the valve V_4 kept closed, the component foreign gas was then admitted into the gas compressor, G, through low temperature traps, B. Liquid nitrogen was used in the traps B for helium and nitrogen gases, and liquid oxygen was used for argon gas. The gas compressor was of mercury-column type and the compression was achieved by means of a column of mercury driven by a hand-operated Aminco oil pump in conjunction with a pressure intensifier. When the required pressure of the foreign gas was reached, the first charge of the foreign gas was then introduced into the absorption cell, which

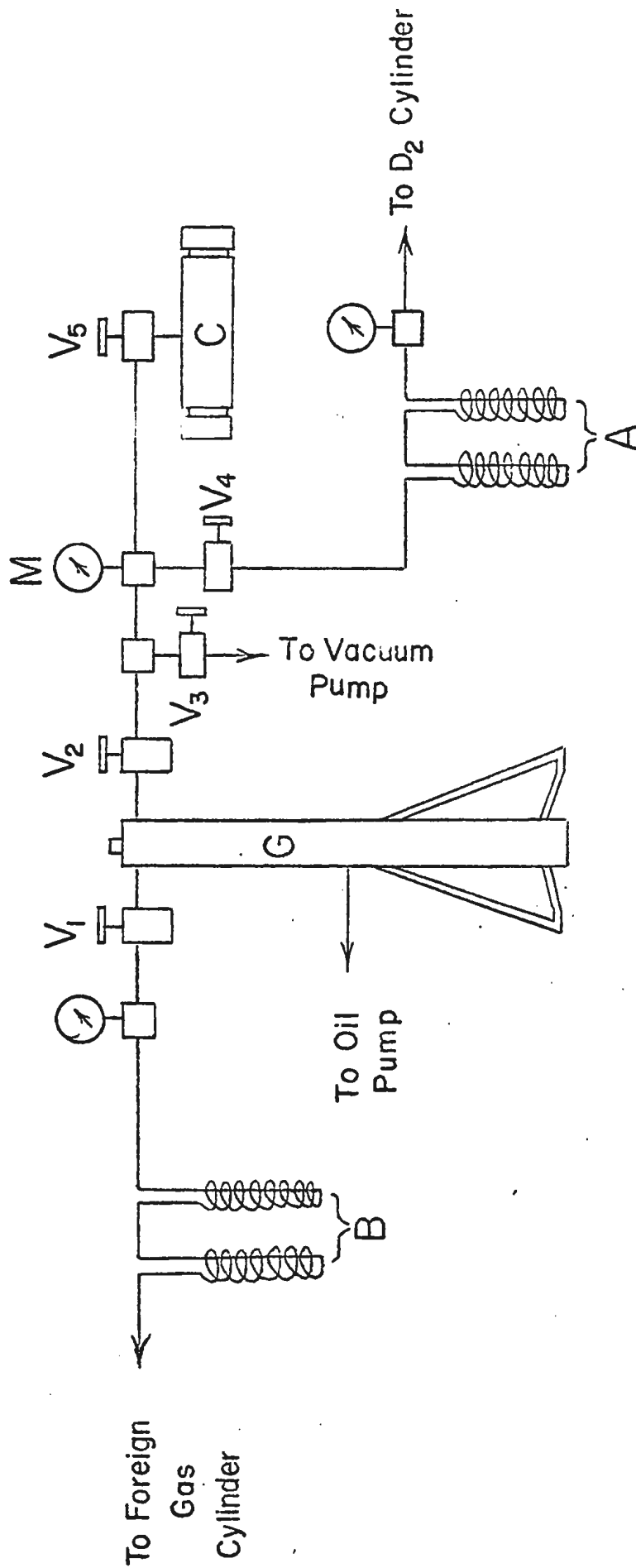


Fig. 4 High pressure gas system.

contained the deuterium gas already, in a way of two or three short pulses controlled by the valve V_5 . Reading of the pressure of the gas mixture inside the cell was taken with the Bourdon tube-type pressure gauge, M, which was calibrated against a dead-weight pressure balance up to a maximum of 20,000 psi. The length of the steel capillary tubing connecting the valve V_5 and the cell was made short so that the possible experimental error caused by the imperfect mixing of gases inside the capillary tubing became negligible. The short pulsing method employed in introducing the foreign gas prevented the possible back diffusion of deuterium gas from the cell.

It was observed that the introduction of foreign gas into the cell caused the signal to fall off, and the signal then returned to the original level after about 10-20 min. Before taking the final recorder trace, several trial traces were taken to ensure a complete mixing of the gases inside the cell. This procedure was repeated for different deuterium-foreign gas mixtures with the same partial density of deuterium. The highest total pressure used in the present study was approximately 1,200 atm.

The partial (base) density of deuterium, ρ_a , was directly determined from the isothermal data by Michels and Goudekt (1941). Three different base densities of deuterium, (53.8, 109, and 138 Amagat) were used for the deuterium-helium mixtures; four (41.5, 44.5, 95, and 134.5 Amagat) for the deuterium-argon mixtures; and three, (21, 33, and 87.5 Amagat) for the deuterium-nitrogen mixtures. The

densities used were expressed in Amagat units of density, which is defined as the ratio of the density at a given pressure and temperature to the density at N.T.P.

To determine the partial density of a foreign gas, ρ_b , the following interpolation method was used. First by assuming the partial pressure of the component gases were additive, the approximate partial pressure of foreign gas was obtained by subtracting the partial pressure of deuterium from the total pressure of the mixture. The approximate partial density of foreign gas, ρ_b' , was then obtained using available isothermal data. (Michels and Wouters (1941) and Hare (1955) for helium; Michels, Wijker and Wijker (1949) for argon; Michels, Wouters and de Boer (1934, 1936) for nitrogen.) Hence the approximate mixture ratio, $\beta' = \rho_b' / \rho_a$, could be calculated. Finally using the equation

$$(1) \quad \rho_b = \frac{1}{1 + \beta'} \left\{ (\rho_a)_P + \beta' (\rho_b)_P \right\} - \rho_a,$$

the partial density, ρ_b , of foreign gas was determined. Here $(\rho_a)_P$ and $(\rho_b)_P$ are the densities of deuterium and foreign gas respectively at the mixture pressure, P, which may be obtained directly from the isothermal data.

For calculating the partial density of a foreign gas in a mixture, a similar method was used by Cho (1963) and it was found that the above method was accurate enough within the limits of experimental error.

CHAPTER III

RESULT AND DISCUSSION

Absorption Profiles

In Fig. 5, a set of enhancement profiles of the induced fundamental absorption band of deuterium in deuterium-helium mixtures, with a constant base density (109 Amagat) of deuterium, is presented for a series of partial density of He. The positions of the band origin ν_0 and the O(4), O(3), O(2), S(0), S(1), S(2), S(3) and S(4) lines, as calculated from the molecular constants of the free molecule determined from the Raman spectrum of gaseous deuterium (Stoicheff 1957) are marked on the frequency axis. The main feature of these profiles is the splitting of the Q branch into two well-resolved components with the minima occurring at the band origin ν_0 . These components at the lower and higher frequency sides of ν_0 are respectively designated as Q_P and Q_R . Similar splitting of the Q branch into two components has already been observed in the induced fundamental band of hydrogen (Chisholm and Welsh 1954) and that of pure deuterium (Reddy and Cho 1965), and has been explained as due to the exchange between the vibrational energy of the absorbing molecules and the kinetic energy of colliding pairs of molecules in a short-range interaction. The separation between the peaks of the components Q_P and Q_R , shows a pronounced dependence on the density of the mixtures. It increases as the density of the mixtures increases. Quantitative discussion of this separation will be presented in Chapter 5. The

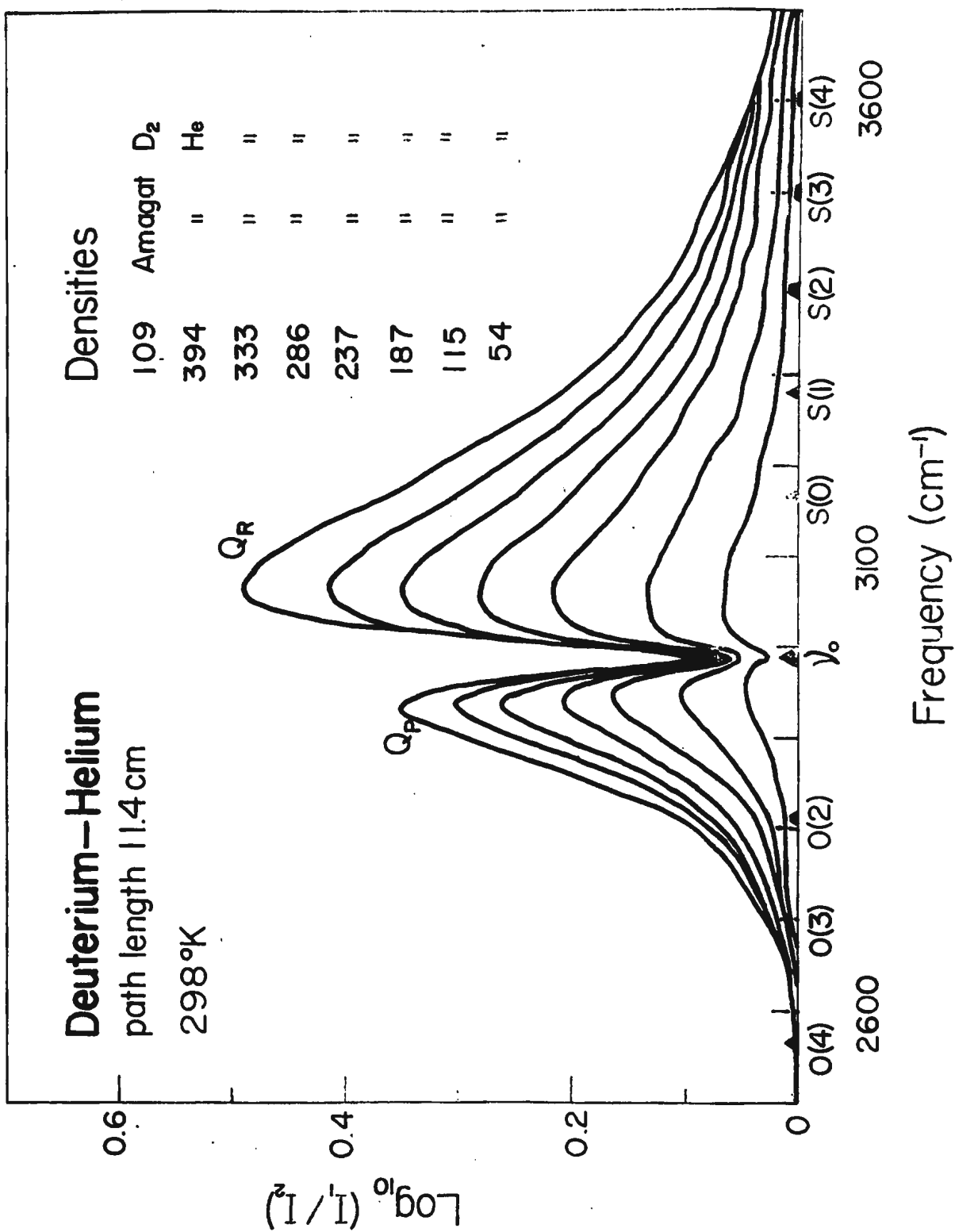


Fig. 5. Observed pressure-induced fundamental absorption band of deuterium in deuterium-helium mixtures.

position of the minimum between the Q_P and Q_R components in each contour shows no appreciable change with the density of the mixtures. As can be seen in Fig. 5 no indication of the existence of any absorption peaks corresponding to the S and O lines could be observed in the contours of deuterium-helium mixtures.

In Figs. 6 and 7 representative sets of the observed enhancement profiles of the band in deuterium-argon and deuterium-nitrogen mixtures, respectively, are presented. As can easily be seen in Fig. 6 the contours in deuterium-argon mixtures show a clear indication of several absorption peaks which agree well with the calculated positions of the O and S lines, in addition to the broad Q_P and Q_R peaks which are similar to those observed in deuterium-helium mixtures. Among the absorption peaks corresponding to the O and S lines, only the S(2) peak is fairly well resolved. The Q_Q peak which has been observed in the fundamental band of hydrogen in hydrogen-argon mixtures at high pressures was not observed in the present investigation, because the range of pressures used was probably too low to make a similar peak appear. The contours in deuterium-nitrogen mixtures, presented in Fig. 7 show a similar appearance as the contours in deuterium-argon mixtures, although the absorption peaks corresponding to the O and S lines are somewhat less pronounced as those in deuterium-argon mixtures.

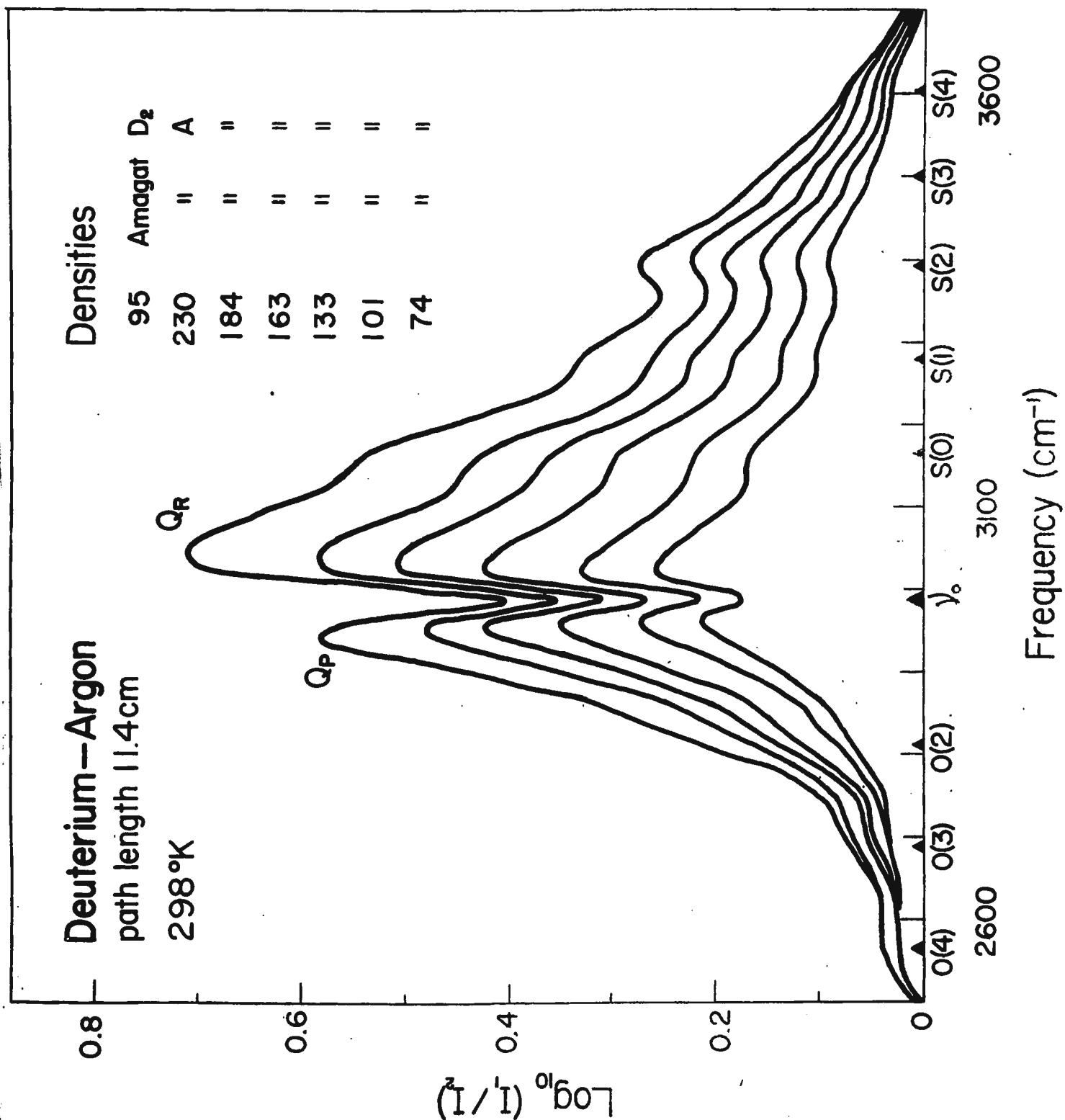


Fig.6 • Observed pressure-induced fundamental absorption band of deuterium in deuterium-argon mixtures.

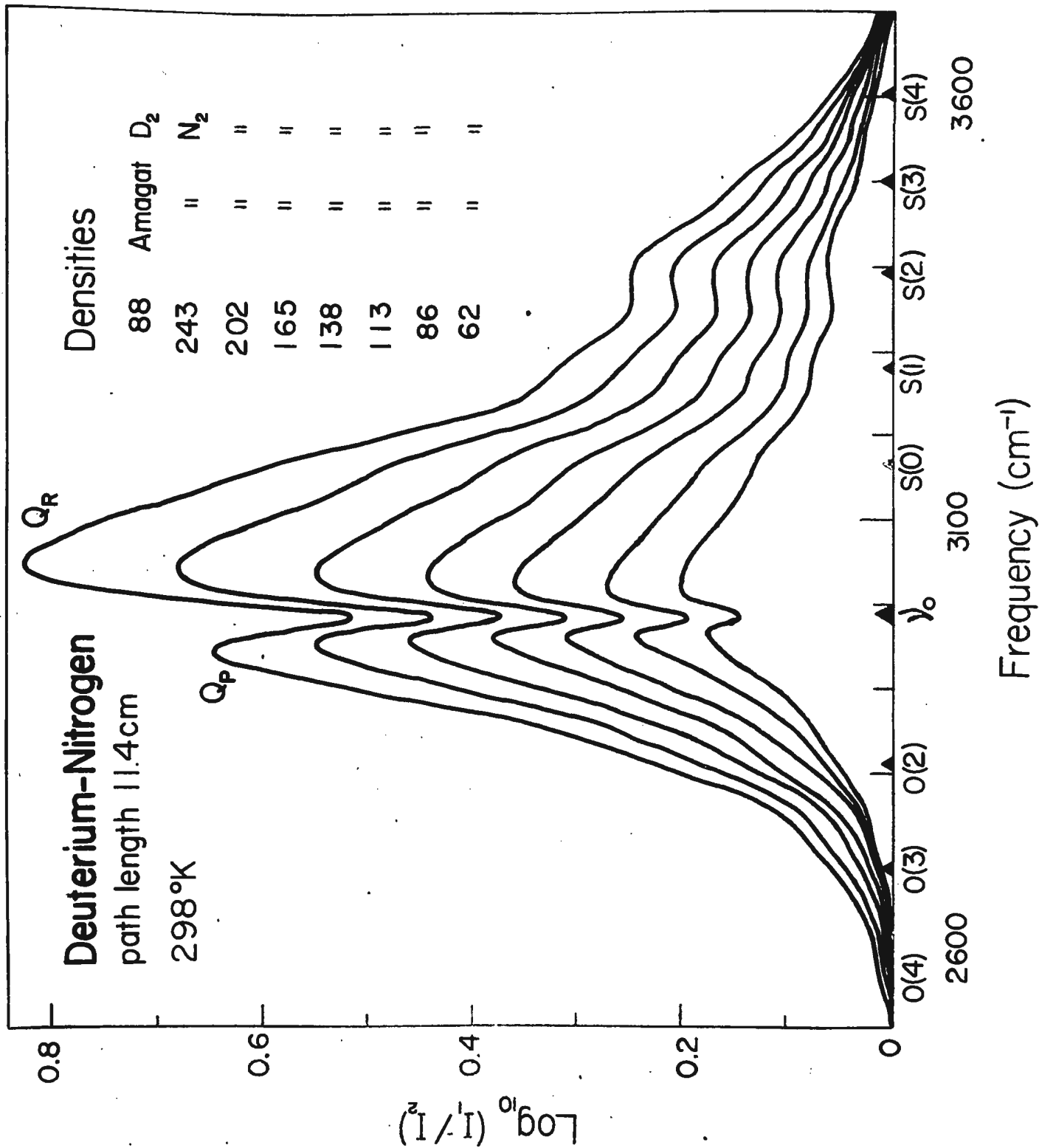


Fig. 7. Observed pressure-induced fundamental absorption band of deuterium in deuterium-nitrogen mixtures.

For the purpose of comparison, the absorption contours of deuterium-helium, deuterium-argon and deuterium-nitrogen mixtures are presented collectively in Fig. 8, together with the contour of pure deuterium which was obtained by Reddy and Cho (1965). The contours in Fig. 8 were chosen in such a way that the product of partial densities, $\rho_a \rho_b$ for deuterium-foreign gas mixtures and ρ_a^2 for pure deuterium, give approximately the same value for each contour. Moreover, the contours of deuterium-foreign gas mixtures in Fig. 8 were chosen to represent approximately the same partial density of deuterium (~ 90 Amagat). The products of partial densities were kept approximately constant in order to compare the overall absorptions arising from the binary collisions between the molecules involved. This is based on the assumption that the main contribution to the absorption arises from the dipole moment induced during binary collisions. Upon an examination of these contours the following observations were made:

- (1) The Magnitude of the total absorption decreases in the following order: deuterium-nitrogen, deuterium-argon, deuterium-deuterium and deuterium-helium binary systems.
- (2) The absorption peaks corresponding to the S and O branches are most pronounced in deuterium-argon mixtures and least pronounced in deuterium-deuterium mixtures, and no indication of such peaks in deuterium-helium mixtures.

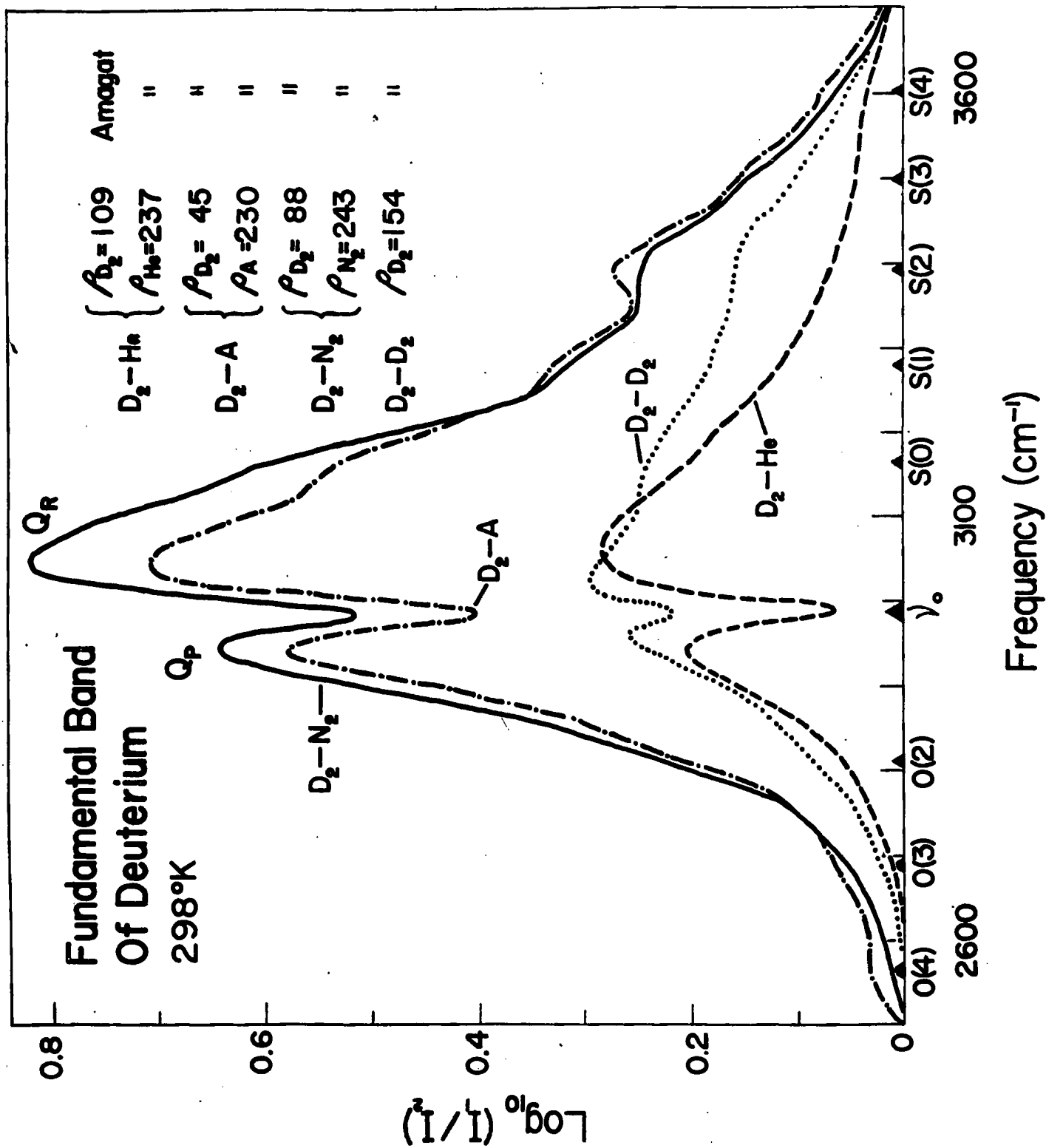


Fig. 8. Absorption contours of the pressure-induced fundamental band of deuterium for various perturbing molecules at room temperature.

- (3) The splitting of the Q branch is least pronounced in deuterium-deuterium mixtures.

A detailed discussion of the absorption profiles will be given later.

The Absorption Coefficients

The observed enhancements in the integrated absorption coefficient of the band in deuterium-foreign gas mixtures are summarized in Table I(a), I(b), and I(c). These results are also graphically represented in Fig. 9 where $(1/\rho_a\rho_b) (\int \alpha d\nu)_{\text{enhancement}}$ was plotted against ρ_b for each of deuterium-helium, deuterium-argon, and deuterium-nitrogen mixtures. These plots seem to represent straight lines; the straight lines drawn in the figure were obtained by the least square method. It is therefore concluded that the enhancement for each mixture may be expressed by the equation

$$(2) \quad (\int \alpha d\nu)_{\text{enhancement}} = \alpha_{1b} \rho_a \rho_b + \alpha_{2b} \rho_a \rho_b^2,$$

where α_{1b} and α_{2b} are the binary and ternary absorption coefficients respectively of a deuterium-foreign gas mixture. The observed coefficients α_{1b} and α_{2b} , determined by the least square method, are presented in Table II. The ranges of error indicated in Table II are the computed standard deviations. For the purpose of comparison, the binary and ternary absorption coefficients of pure deuterium which were obtained by Reddy and Cho (1965), and those of hydrogen and hydrogen-foreign gas mixtures obtained by Hare and Welsh (1958), are also presented in Table II. It can be noted that the values of the absorption coefficients of the fundamental band of deuterium in the

Table I (a)
Summary of Results
D₂ - He Mixture

ρ_{D_2} (Amagat)	ρ_{He} (Amagat)	$\int \alpha d\nu$ (cm ⁻¹ /cm)	ρ_{D_2} (Amagat)	ρ_{He} (Amagat)	$\int \alpha d\nu$ (cm ⁻¹ /cm)
138.0	44.4	5.39	109.0	285.8	28.45
"	94.6	10.92	"	333.3	32.94
"	144.7	17.30	"	39.40	39.09
"	192.4	23.20	53.8	152.0	6.74
"	272.4	30.95	"	261.5	12.05
"	339.3	39.84	"	346.4	17.75
109.0	53.7	4.90	"	431.2	22.33
"	114.8	10.86	"	524.3	27.60
"	179.8	17.34	"	590.6	31.53
"	236.6	23.02	"	662.0	35.73

Table I (b)

Summary of Results

D₂ - A Mixture

ρ_{D_2} (Amagat)	ρ_A (Amagat)	$\int \alpha d\nu$ (cm ⁻¹ /cm)	ρ_{D_2} (Amagat)	ρ_A (Amagat)	$\int \alpha d\nu$ (cm ⁻¹ /cm)
134.5	34.4	12.85	44.5	56.7	6.28
"	47.6	17.60	"	103.2	13.85
"	67.1	23.99	"	144.8	20.51
"	89.1	32.39	"	189.7	26.93
"	115.6	42.15	"	240.6	32.91
"	145.5	55.51	"	300.6	41.02
95.0	73.9	21.80	"	350.6	52.11
"	101.0	28.10	41.5	79.3	9.88
"	133.4	37.20	"	136.8	16.59
"	163.0	45.10	"	196.3	23.48
"	183.6	53.10	"	244.5	30.71
"	229.8	64.80	"	295.1	37.82
"	263.5	77.10	"	360.2	48.49

Table I (c)
 Summary of Results
 D₂ - N₂ Mixture

ρ_{D_2} (Amagat)	ρ_{N_2} (Amagat)	$\int \alpha d\nu$ (cm ⁻¹ /cm)	ρ_{D_2} (Amagat)	ρ_{N_2} (Amagat)	$\int \alpha d\nu$ (cm ⁻¹ /cm)
87.5	62.0	16.48	33.0	304.5	36.04
"	85.5	21.99	"	349.8	41.90
"	112.5	29.21	"	381.8	47.35
"	137.6	36.80	21.0	157.4	11.37
"	165.1	45.70	"	203.2	14.49
"	202.4	57.05	"	256.0	18.75
"	243.1	69.46	"	308.4	22.63
33.0	134.5	14.62	"	362.5	26.66
"	158.8	17.70	"	402.7	29.58
"	209.4	24.36	"	419.9	31.53
"	263.7	30.85			

Fig. 9 The relation between the enhancement integrated absorption coefficients of the fundamental band of D₂ and the partial density of foreign gas in D₂-foreign gas mixtures.

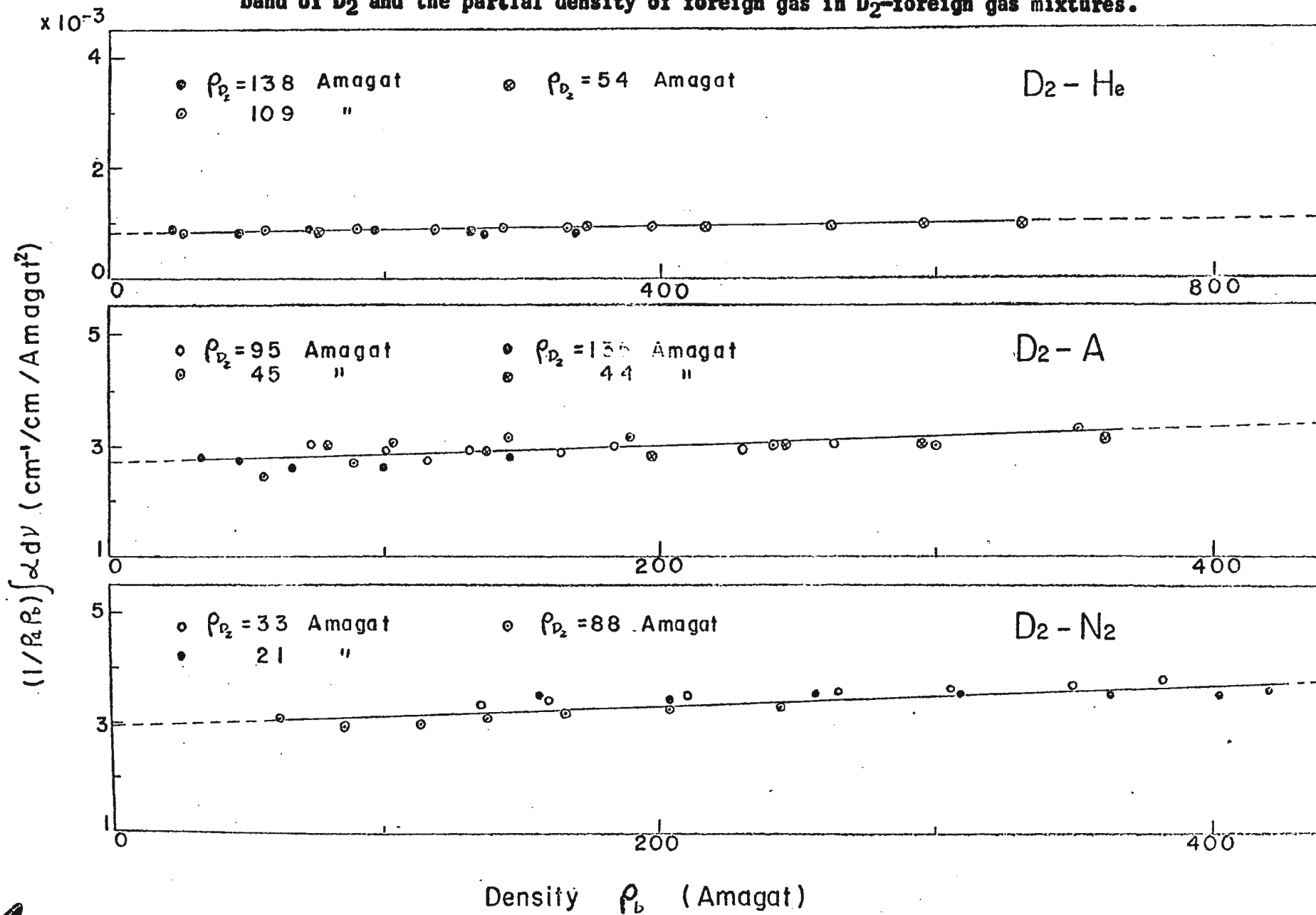


Table II

Observed absorption coefficients of the fundamental induced
band of deuterium in deuterium-foreign gas mixtures.

Mixture	Binary absorption coefficient ($10^{-3} \text{ cm}^{-2} \text{ Amagat}^{-2}$)	Ternary absorption coefficient ($10^{-6} \text{ cm}^{-2} \text{ Amagat}^{-3}$)
$\text{D}_2 - \text{He}$	$\alpha_{1b} = 0.82 \pm 0.01$	$\alpha_{2b} = 0.27 \pm 0.03$
($\text{H}_2 - \text{He}$)	(1.1)	(0.55)
$\text{D}_2 - \text{A}$	$\alpha_{1b} = 2.71 \pm 0.04$	$\alpha_{2b} = 1.5 \pm 0.2$
($\text{H}_2 - \text{A}$)	(4.1)	(3.9)
$\text{D}_2 - \text{N}_2$	$\alpha_{1b} = 2.95 \pm 0.05$	$\alpha_{2b} = 1.79 \pm 0.19$
($\text{H}_2 - \text{N}_2$)	(5.4)	(5.5)
$\text{D}_2 - \text{D}_2^*$	$\alpha_{1a} = 1.06 \pm 0.02$	$\alpha_{2a} = 0.8 \pm 0.2$
($\text{H}_2 - \text{H}_2$)	(2.4)	(1.1)

Values in brackets were obtained by Hare and Welsh (1958).

*Values were obtained by Reddy and Cho (1965).

binary mixtures are approximately one half of the corresponding values obtained for the fundamental band of hydrogen.

The empirical relation given by equation (2) above contain second-order and third-order terms in ρ_a and ρ_b . While the second-order term, $\alpha_{1b}\rho_a\rho_b$, may be interpreted as the contribution arising from the binary collisions between one deuterium molecule and one foreign gas molecule to the enhancement absorption, the third-order term, $\alpha_{2b}\rho_a\rho_b^2$, has been interpreted by previous authors (e.g. Hare and Welsh 1958) as due to three ternary effects. They are: (a) the finite volume effect, (b) ternary collisions, and (c) the change of molecular polarizability with pressure. The effect of finite volume was discussed by Chisholm and Welsh (1954), and an expression for α_2/α_1 in terms of the molecular diameter, D , of the perturbing molecule was derived from a simple theory. Qualitative considerations have shown that ternary and higher order collisions would annul to some extent the contribution of the binary collisions to the absorption when a particular absorbing molecule is surrounded by a symmetrical configuration of the perturbing molecules. This has been referred to as "cancellation effect". The decrease in molecular polarizabilities at high densities which was predicted by quantum mechanical considerations (Michel, de Boer, and Bijl 1937, de Groot and ten Seldam 1947), would lower the absorption coefficient to some extent, but the magnitude of the effect, which is difficult to estimate is probably very small for H_2 . It may also be noted that

another possible ternary term $\alpha_{2ab} \rho_a^2 \rho_b$ is missing in equation (2). The absence of such a term is probably due mainly to the limited experimental accuracy in the deduction of the present results, and to the smallness of the ternary coefficient α_{2b} .

Based on the consideration of the "finite volume effect", an expression relating the absorption coefficients and the molecular diameter, D , as derived by Chisholm and Welsh (1954) is given by

$$(3) \quad \alpha_{2b}/\alpha_{1b} = (4/3) \pi n_0 D^3,$$

where n_0 is the Loschmidt's number. Using the observed values of α_{1b} and α_{2b} the molecular diameter, D , of the perturbing gas were calculated by means of (3) and are given in Table III. Values of σ , the distance of nearest approach of two molecules which collide with zero initial relative kinetic energy, and obtained from the kinetic theory of gases, are presented in the last column of the same table. It can be seen that values calculated from the absorption coefficients are approximately one half of those obtained from the kinetic theory calculations. This discrepancy may probably be due to the cancellation effect. The same kind of discrepancy has been found by Chisholm and Welsh (1954) in the case of H_2 -foreign gas mixtures.

Table III

Molecular Diameter of Perturbing Gas

Perturbing gas	Molecular diameters	
	D Å	σ^* Å
He	1.44	2.74
A	1.70	3.17
N ₂	1.75	3.31

*Calculated from the values given in "Molecular Theory of Gases and Liquids" by Hirschfelder, Curtis and Bird (1954)

CHAPTER IV
THEORY AND CALCULATION

Among the theories of the induced infrared absorption of homonuclear diatomic molecules which have been proposed by various authors, the one developed by Van Kranendonk (1957, 1958) has been proved to be the most adequate in explaining the induced fundamental absorption band of hydrogen (e.g. Hunt and Welsh 1964). In the present Chapter, an outline of the theory by Van Kranendonk is given and an attempt is made to apply the theory for the explanation of the experimental results obtained in the present investigation. The main purpose of the application of the theory here is to study the contributions arising from the effects of the long-range quadrupole interaction and the short-range overlap interaction separately from the experimental results.

The specific integrated absorption coefficients of a binary gas mixture in terms of partial densities can be given by the equation

$$(4) \quad \tilde{\alpha} = \frac{1}{\tilde{\rho}_a} \int \tilde{A} d\nu' = \tilde{\alpha}_{1a} \tilde{\rho}_a + \tilde{\alpha}_{1b} \tilde{\rho}_b + \tilde{\alpha}_{2a} \tilde{\rho}_a^2 + \tilde{\alpha}_{2b} \tilde{\rho}_b^2 + \tilde{\alpha}_{2ab} \tilde{\rho}_a \tilde{\rho}_b + \text{-----}$$

where \tilde{A} is the absorption coefficient per wave-length, ν' is the frequency in sec^{-1} , $\tilde{\rho}_a$ and $\tilde{\rho}_b$ are the number densities, (N/V) , of the gas components a and b respectively. In equation, (4) $\tilde{\alpha}_{1a}$ and $\tilde{\alpha}_{2a}$ are the binary and ternary absorption coefficients of the

absorbing gas a; $\tilde{\alpha}_{1b}$ and $\tilde{\alpha}_{2b}$ the binary and ternary absorption coefficients arising due to a mixture of the absorbing molecules and the perturbing molecules; $\tilde{\alpha}_{2ab}$ is the mixed ternary absorption coefficient. Since in the present investigation only enhancement absorptions are considered, the enhancement absorption coefficient, $\tilde{\alpha}_{\text{enhancement}}$, can be expressed as follows

$$(5) \quad \tilde{\alpha}_{\text{enhancement}} = \tilde{\alpha}_{1b} \tilde{\rho}_b + \tilde{\alpha}_{2b} \tilde{\rho}_b^2 + \tilde{\alpha}_{2ab} \tilde{\rho}_a \tilde{\rho}_b + \text{-----}$$

The absorption coefficients α_{1b} and α_{2b} given in the empirical equation (2) are related to those given in equation (5) by the following equations.

$$(6) \quad \begin{aligned} \tilde{\alpha}_{1b} &= c \alpha_{1b} (V_0^2 / \bar{\nu} N_A^2), \\ \tilde{\alpha}_{2b} &= c \alpha_{2b} (V_0^2 / \bar{\nu} N_A^2), \end{aligned}$$

where

$$(7) \quad \bar{\nu} = \int \alpha(\nu) d\nu / \int \nu^{-1} \alpha(\nu) d\nu .$$

Here V_0 is the molecular volume at N.T.P., N_A is Avagadro's number, and ν is expressed in cm^{-1} . $\bar{\nu}$ for the deuterium fundamental band in the mixtures studied was found to be approximately constant for various mixtures and equal to 3140 cm^{-1} . It may be noted that the coefficient α_{2ab} could not be determined in the present investigation.

The binary absorption coefficient, α_{1b} , may be considered as arising from the dipole moment induced in the absorbing molecule during

the binary collision between a pair of one absorbing and one perturbing molecules. In the moderate range of pressures, such as the one used in the present investigation, the contribution of the binary coefficient to the total absorption intensity of the band is predominant over other contributions arising from the higher order terms. In the present investigation, it was estimated that approximately 90% of the total absorption intensity was due to the binary effect even at the highest partial densities used. The theory of the binary absorption coefficient developed by Van Kranendonk will be given in the section below. The ternary absorption coefficient, $\tilde{\alpha}_{2b}$, consists of a sum of three terms: the first term gives the contribution arising from the density dependence of the pair distribution function; the second term is due to an interference effect between the moments induced in the pairs of molecules (1, 2) and (1, 3); and the third term is due to the non-additive contribution to the moment induced by two perturbing molecules in a triple collision of the type a-b-b.

The Theory of Binary Absorption Coefficient in Mixtures

The binary absorption coefficient of a definite rotational branch B of the fundamental band in a binary mixture is given by

$$(8) \quad \tilde{\alpha}_{1b}^{(B)} = \mathcal{K} \sum^{(B)} P_1 P_2 \int |\vec{M}(\vec{R}_{12})|^2 g_0(\vec{R}_{12}) d\vec{R}_{12} .$$

Here \mathcal{K} is defined as $\mathcal{K} = \pi/3 m_0 \nu_0$, m_0 and ν_0 being the reduced mass and the frequency of the molecular oscillation, respectively and, P_1 and P_2 , the normalized Boltzmann factors for molecule 1 of gas a

and molecule 2 of gas b respectively. \vec{R}_{12} is the vector representing the intermolecular distance and $g_0(\vec{R}_{12})$ the pair distribution function arising from ab pair molecules. $\vec{M}(\vec{R}_{12})$ is the induced moment of a pair molecules (1,2). The induced moment contains two additive parts: a short-range angle-independent overlap moment, of strength \mathcal{F} and range ρ , which decreases exponentially with increasing intermolecular distance R; and a long-range angle-dependent moment which is proportional to R^{-4} . The long-range moment is assumed to be dependent on the derivatives of the quadrupole moment and the average polarizability of the absorbing molecule at the equilibrium position, Q_1' and α_1' respectively, and the quadrupole moment and the average polarizability of the perturbing molecule, Q_2 and α_2 respectively. Based on the 'exp-4' model for the induced moment, the components of $\vec{M}(\vec{R}_{12})$ are assumed to be as follows:

$$(9) \quad \begin{cases} M_0 = \mathcal{F} \exp(-R/\rho) + (3/2) \{ Q_1' \alpha_2 (3 \cos \theta_1 - 1) - Q_2 \alpha_1' (3 \cos \theta_2 - 1) \} R^{-4}, \\ M_{+1} = (3/\sqrt{2}) (Q_1' \alpha_2 e^{i\varphi_1} \sin \theta_1 \cos \theta_1 - Q_2 \alpha_1' e^{i\varphi_2} \sin \theta_2 \cos \theta_2) R^{-4}, \\ M_{-1} = (3/\sqrt{2}) (Q_1' \alpha_2 e^{-i\varphi_1} \sin \theta_1 \cos \theta_1 - Q_2 \alpha_1' e^{-i\varphi_2} \sin \theta_2 \cos \theta_2) R^{-4}, \end{cases}$$

where θ_1, φ_1 and θ_2, φ_2 specify the polar angles of the internuclear axes of the molecules 1 and 2, relative to a coordinate frame xyz, the z-axis of which lies along the vector \vec{R}_{12} that connects the centre of mass of molecule 1 to that of molecule 2. In equations (9), $Q_1' = (\partial Q_1 / \partial r_1)_0$, and $\alpha_1' = (\partial \alpha_1 / \partial r_1)_0$, where r_1 being the inter-

nuclear distance of the absorbing molecules. By substituting equations (9) into (8), the expressions for the binary absorption coefficients for the O, Q and S branches of the induced fundamental band in the mixture have been derived by Van Kranendonk (1958) as follows:

$$(10) \quad \tilde{\alpha}_{1b} [O(J)] = \mu_1^2 \underline{J} \tilde{r} \cdot L_2 [O(J)] ;$$

$$(11) \quad \tilde{\alpha}_{1b} [Q(J)] = (\lambda^2 \underline{1} + \mu_2^2 \underline{J}) \tilde{r} \cdot L_0 [Q(J)] \\ + \mu_1^2 \underline{J} \tilde{r} \cdot L_2 [Q(J)] ;$$

$$(12) \quad \tilde{\alpha}_{1b} [S(J)] = \mu_1^2 \underline{J} \tilde{r} \cdot L_2 [S(J)] ;$$

where J is the rotational quantum number. The above expressions may also be used to calculate the binary absorption coefficient for each individual line. The corresponding expressions for the case in which the perturbing molecules are monatomic can be obtained from (10), (11) and (12) by putting $\mu_2 = 0$.

In equations (10), (11) and (12) the dimensionless parameters λ , μ_1 , μ_2 are defined as

$$(13) \quad \lambda = (\mathcal{E}/e) \exp(-\sigma/\rho),$$

$$(14) \quad \mu_1 = Q_1' \alpha_2/e \sigma^4, \quad \mu_2 = \alpha_1' Q_2/e \sigma^4,$$

where σ is the intermolecular distance R for which the intermolecular potential is zero and e is the value of the electronic charge. \tilde{r} is

defined by

$$(15) \quad \tilde{\gamma} = \pi e^2 \sigma^3 / 3 m_0 \nu_0,$$

where m_0 and ν_0 are the reduced mass of the absorbing molecule and the frequency of the molecular vibration respectively. The radial distribution integrals \underline{I} and \underline{J} are given by

$$(16) \quad \underline{I} = 4\pi \int_0^\infty \exp \{ - 2(x-1) \sigma / \rho \} g_0(x) x^2 dx$$

and

$$(17) \quad \underline{J} = 12 \pi \int_0^\infty x^{-8} g_0(x) x^2 dx,$$

where $x = R/\sigma$, and $g_0(x)$ is the low-density limit of the pair distribution function. In the equations (10), (11) and (12), $L_\lambda(B)$ is defined as

$$(18) \quad L_\lambda(B) = \sum_{J, J'}^{(B)} P_a(J) L_\lambda(J, J'),$$

where $P_a(J)$ is the Boltzmann factor for the absorbing molecule with rotational quantum number J , normalized in such a way that

$$(19) \quad \sum_{J=0}^\infty (2J+1) P_a(J) = 1.$$

The quantities $L_\lambda(J, J')$ are Racah coefficients, the non-vanishing values of $L_\lambda(J, J')$ for $\lambda = 0$ and 2 , are given by

$$\begin{aligned}
 L_0(J, J) &= 2J + 1, \\
 L_2(J, J-2) &= 3(J-1) / 2(2J-1) \\
 L_2(J, J) &= J(J+1)(2J+1) / (2J-1)(2J+3), \\
 L_2(J, J+2) &= 3(J+1)(J+2) / 2(2J+3).
 \end{aligned}
 \tag{20}$$

The total binary absorption coefficient, $\tilde{\alpha}_{1b}$, can then be obtained by adding the equations (10), (11) and (12), after the summation over J. Thus

$$\tilde{\alpha}_{1b} = \lambda^2 \underline{\mathbb{I}} \tilde{\gamma} + (\mu_1^2 + \mu_2^2) \underline{\mathbb{I}} \tilde{\gamma}.
 \tag{21}$$

In equation (21) the first term represents the contribution due to the overlap interaction and the second term that due to quadrupole interaction.

Calculations for the Deuterium-Foreign Gas Mixtures

In the present calculations, the quadrupole part, $(\mu_1^2 + \mu_2^2) \underline{\mathbb{I}} \tilde{\gamma}$ in equation (21) is calculated first, using the known molecular parameters of deuterium and foreign gas. From this value and the experimental value of $\tilde{\alpha}_{1b}$ obtained in the present investigation, the overlap part $\lambda^2 \underline{\mathbb{I}} \tilde{\gamma}$ and hence λ^2 are obtained. These calculations were made using the following procedure.

At high temperatures, the pair distribution function $g_0(x)$ in the equation (16) and (17) is equal to $\exp(-V(x)/kT)$ classically, where $V(x)$ is assumed to be the Lennard-Jones intermolecular potential

$$(22) \quad V(x) = 4 \epsilon (x^{-12} - x^{-6}).$$

At intermediate temperatures, $g_0(x)$ may be expanded as an asymptotic series in powers of Plank's constant. The resulting expressions of the above integrals (16) and (17) are expressed in the form

$$\begin{aligned} \underline{I} &= \underline{I}_{c1} - \Lambda^{*2} \underline{I}^{(2)} + \Lambda^{*4} \underline{I}^{(4)} + \text{-----} \\ \underline{J} &= \underline{J}_{c1} - \Lambda^{*2} \underline{J}^{(2)} + \Lambda^{*4} \underline{J}^{(4)} + \text{-----} \end{aligned}$$

where $\Lambda^* = (h^2/2m \epsilon \sigma^2)^{\frac{1}{2}}$, m being the reduced mass of the pair of colliding molecules. For the calculation of \underline{I} , the accurate relationship between ρ and σ must be known. The empirical determination of this relationship may only be possible by studying the temperature variation of the parameter Λ^2 . Since such experimental results are not available for the deuterium fundamental band the relationship used by Van Kranendonk and Kiss (1959) for hydrogen, $\rho = 0.126 \sigma$, was assumed to be applicable for deuterium as well in the present calculations. They have calculated numerically the integrals \underline{I}_{c1} , $\underline{I}^{(2)}$, $\underline{I}^{(4)}$, \underline{J}_{c1} , $\underline{J}^{(2)}$ and $\underline{J}^{(4)}$ for a number of reduced temperatures. $T^* = \frac{kT}{\epsilon}$. Using these values for the integrals and the corresponding values of Λ^* for each mixture, the values of \underline{I} and \underline{J} for different deuterium-foreign gas mixtures at room temperature were calculated. These calculated values of \underline{I} and \underline{J} and other molecular parameters used in the present investigation are given in Table IV. The quantities

Table IV

Molecular data for calculation of absorption
coefficients for deuterium-foreign gas mixtures

Mixture	$\sigma^{(a)}$ (Å)	$\epsilon/k^{(a)}$ (°K)	$T^* = \frac{298}{\epsilon/k}$	Λ^*	$\underline{I}^{(b)}$	$\underline{J}^{(b)}$	$\tilde{\gamma} \times 10^{-32}$ (cm ⁶ sec ⁻¹)	α/a_0^3	Q/ea_0^2
D ₂ - He	2.742	19.44	15.33	1.805	6.32	15.33	3.29	1.4 ^(c)	-
D ₂ - A	3.167	66.58	4.48	0.626	2.85	12.16	5.07	11.1 ^(c)	-
D ₂ - N ₂	3.313	59.30	5.03	0.646	3.04	12.29	5.80	11.8 ^(c)	1.1 ^(d)

(a) Hirschfelder, J.O., Curtis, F.C., Bird, R.B., Molecular Theory of Gases and Liquids, Wiley, New York, 1954.

(b) ρ/σ is assumed to be 0.126. Ref: Van Kranendonk, J., and Kiss, Z.J., Can. J. Phys. 37, 1187 (1959).

(c) See Van Kranendonk, J., Physica, 24, 347 (1958).

(d) See Reddy, S.P., and Cho, C.W. Can. J. Phys. (in Press).

Q' and α' of deuterium are assumed to be the same as those of hydrogen, i.e. $Q'/ea_0 = 0.44$, $\alpha'/a_0^2 = 3.9$ (Hunt and Welsh 1964).

The results of the calculations are summarized in Table V. In this table the quadrupole part and the overlap part of the binary absorption coefficient as calculated from the observed binary absorption coefficient for deuterium-foreign gas mixtures are presented. The parameter λ^2 and the overall percentage of each part in the observed coefficient also presented in the same table. For the purpose of comparison the corresponding values for pure deuterium are shown in Table V. Discussion of these results in conjunction with the shape of the observed absorption contours will be given in the next chapter.

Finally using the equations (10), (11), and (12) the binary absorption coefficients of individual lines of the O and S branches, and the quadrupole part of the Q branch were calculated. Since the contribution of the overlap part $\lambda^2 \underline{I} \tilde{\gamma}$ to the band is assumed to give rise solely to the Q branch the overlap part of the Q branch in each mixture can be obtained by subtracting the entire quadrupole part from the total binary absorption coefficient. The results are summarized in Table VI. The results presented in Table VI will also be discussed in the next chapter where an analysis of the observed absorption contours will be presented.

Table V

Electron overlap and molecular quadrupole parts of the binary
absorption coefficients of the induced fundamental band of D₂.

Mixture	$\alpha_{1b} \times 10^3$ (cm ⁻¹ /cm Agt ²)	$\tilde{\alpha}_{1b} \times 10^{35}$ (cm ⁶ sec ⁻¹)	Quadrupole part ($u_1^2 + u_2^2$) $\perp \tilde{\Gamma} \times 10^{35}$ (cm ⁶ sec ⁻¹)	Overlap part $\lambda^2 \perp \tilde{\Gamma} \times 10^{35}$ (cm ⁶ sec ⁻¹)	$\lambda^2 \times 10^5$	Percentage	
						Overlap	Quadrupole
D ₂ - He	0.82	1.081	0.037	1.044	5.02	97	3
D ₂ - A	2.71	3.573	0.891	2.682	18.57	75	25
D ₂ - N ₂	2.95	3.890	1.367	2.523	14.30	65	35
D ₂ - D ₂ [*]	1.06	1.398	0.559	0.839	5.21	60	40

*Calculated from the experimental results of Reddy and Cho (1965), by using the values of $\epsilon/k = 37.00^\circ\text{K}$,
 $\sigma = 2.928\text{\AA}$.

Table VI

Binary absorption coefficients of the fundamental band of deuterium ($10^{-35}\text{cm}^6\text{sec}^{-1}$)

Mixture	O(4)	O(3)	O(2)	Q_{overlap}	Q_{quad}	S(0)	S(1)	S(2)	S(3)	S(4)	Total
D ₂ - He	-	-	-	1.04	0.01	0.01	0.01	0.01	-	-	1.08
D ₂ - A	0.02	0.03	0.07	2.68	0.23	0.16	0.11	0.18	0.05	0.04	3.57
D ₂ - N ₂	0.02	0.02	0.06	2.52	0.79	0.15	0.10	0.16	0.04	0.03	3.89
(D ₂ - D ₂) [*]	(0.01)	(0.02)	(0.04)	(0.84)	(0.16)	(0.10)	(0.07)	(0.11)	(0.03)	(0.02)	(1.40)

*Values in brackets were obtained from the values by Reddy and Cho (1965)

CHAPTER V

CONTOUR ANALYSIS

The spectral lines observed in the absorption spectra of gases at high pressures are always broadened. Especially the pressure-induced spectra of otherwise forbidden transitions exhibit a characteristic diffuse appearance which often prevents the study of individual lines.

The pressure broadening of the spectral lines in gaseous mixtures which arise from the allowed transitions may be divided into two parts: one due to the self-broadening resulting from the participation of the translational motion of the absorbing molecules and the other due to the foreign-broadening caused by the translational motion of the foreign molecules. It has been generally understood that this pressure broadening gives rise to the dispersion (Lorentz) line shape for individual spectral lines, the dispersion half-width being sensitive to pressures, and that, in the case of the foreign broadening, the integrated absorption coefficient remains constant at moderate pressures. Although the diffuse appearance of the pressure induced spectra may be considered as due to a similar mechanism as above at first glance, the exchange of energies between a particular transition which gives rise to the absorption, and the relative translational motion of molecules involved is based on a different physical phenomena. The diffuseness of the pressure-induced spectra is due to the modulation

of the induced dipole which gives rise to the absorption by the relative translational motion of the colliding molecules, while the 'ordinary' pressure broadening is due simply to the participation of relative kinetic energy of colliding molecules in the transition without the modulation of dipole moment of the absorbing molecule. The participation of the relative kinetic energy in pressure-induced absorption process leads to two characteristic properties: on one hand the pressure-induced spectral line retains a more or less constant shape, and on the other hand the line profile has a marked temperature dependence.

The Absorption Profile of D₂ - He Mixtures

In the induced fundamental band of deuterium the spacings between adjacent rotational lines are reasonably large. However because of the diffuse nature of the vibration-rotation lines of the O and S branches which superimpose on the broad and intense Q branch, a purely empirical separation of these lines from the Q branch of the observed absorption contour at room temperature becomes almost impossible. This difficulty affects, especially, the analysis of absorption contours obtained in the deuterium-argon and deuterium-nitrogen mixtures. The contours of deuterium-helium mixtures differ greatly from those of deuterium-argon and deuterium-nitrogen mixtures. As it was found in Chapter IV, each contour of deuterium-helium mixtures consists mainly of the Q branch which arises from the overlap interaction only (97% of the total intensity). It

is therefore well justified to assume that the absorption contour of deuterium-helium mixtures represent purely the Q branch due to the overlap interactions.

Following the method developed by Hunt and Welsh (1964), each observed contour obtained in deuterium-helium mixtures was analyzed to obtain the dispersion half-width of the Q branch. When the high frequency wing of the Q_R branch of the contour obtained in deuterium-helium mixture was examined, it was found that this wing, in general, formed a part of a dispersion curve which may be expressed by the equation

$$(24) \quad I_+ = I_0 / \left\{ 1 + \left(\frac{\Delta\nu}{\delta} \right)^2 \right\},$$

where I_+ is the intensity at $\nu_0 + \Delta\nu$, I_0 is the fictitious maximum intensity at ν_0 , and δ is the dispersion half-width.

ν_0 is the band origin which coincides with the position of the central minimum of the band. An example of the test which verifies this dispersion shape is given in Fig. 10. In this figure the reciprocal intensity $1/I_+$ is plotted against $(\Delta\nu)^2$. As is seen in the figure the plot can well be represented by a straight line whose intercept is equal to $1/I_0$, and whose slope gives $1/(I_0 \delta^2)$. Therefore, from Fig. 10, one can determine I_0 and δ of the dispersion curve. The dispersion half-width of the contours, δ_{overlap} , was found to be approximately constant for different mixtures and its value is given in Table VII. For the fundamental band of hydrogen in

Fig. 10 Illustration of the dispersion line form for the high-frequency wing of the absorption contour of D₂-He mixture.

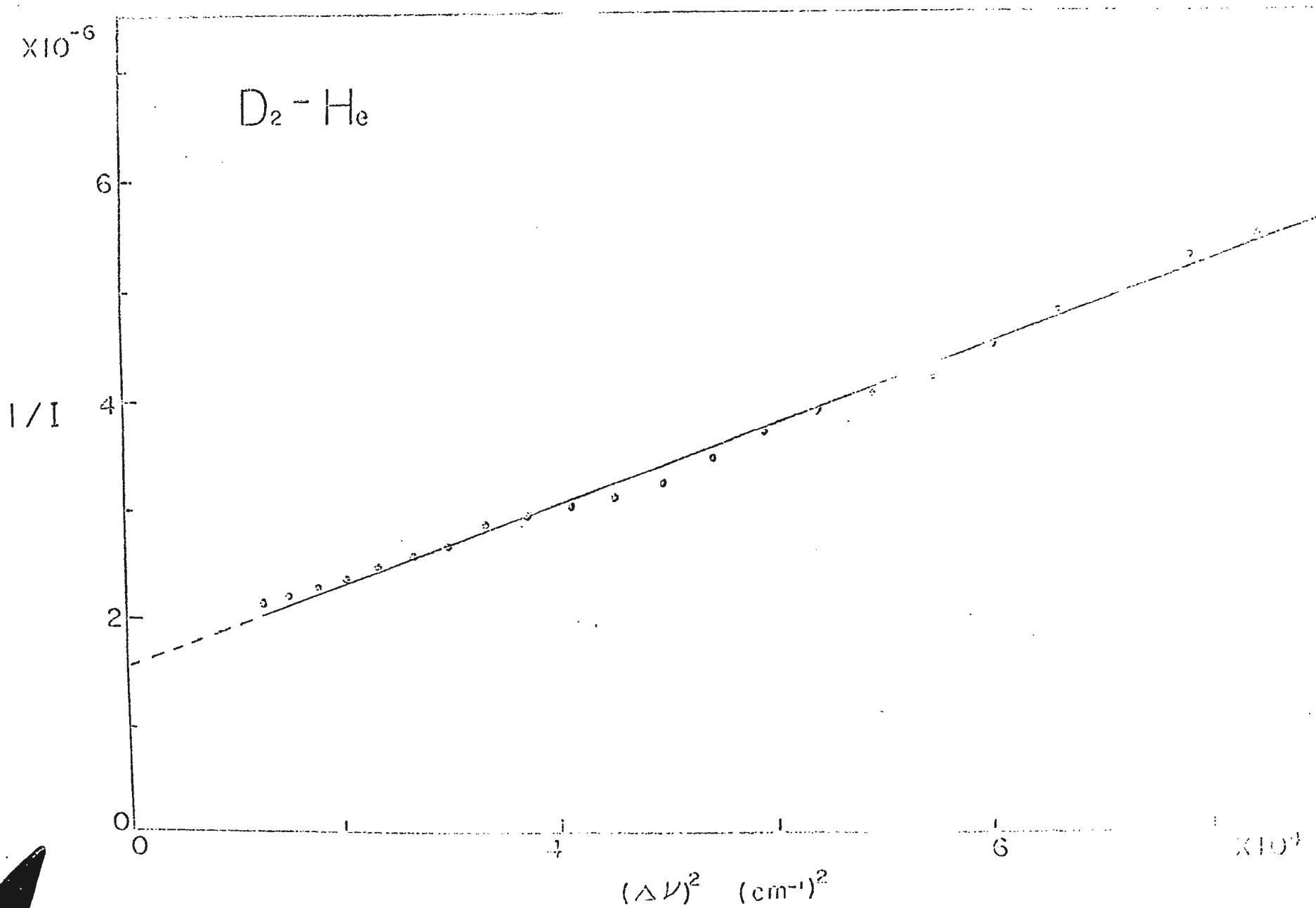


Table VII

Dispersion half-widths of the overlap and quadrupole components

Mixture	T (K ^o)	δ_{overlap} (cm ⁻¹)	δ_{quad} (cm ⁻¹)
D ₂ - He	298	209	-
(H ₂ - He)	(300)	(250)	(-)
D ₂ - A	298	174	65
(H ₂ - A)	(300)	(160)	(110)
D ₂ - N ₂	298	165	63
(H ₂ - N ₂)	(300)	(166)	(110)
D ₂ - D ₂ [*]	298	262	10D
(H ₂ - H ₂)	(300)	(290)	(142)

Values in brackets were obtained by Hunt and Welsh (1964)

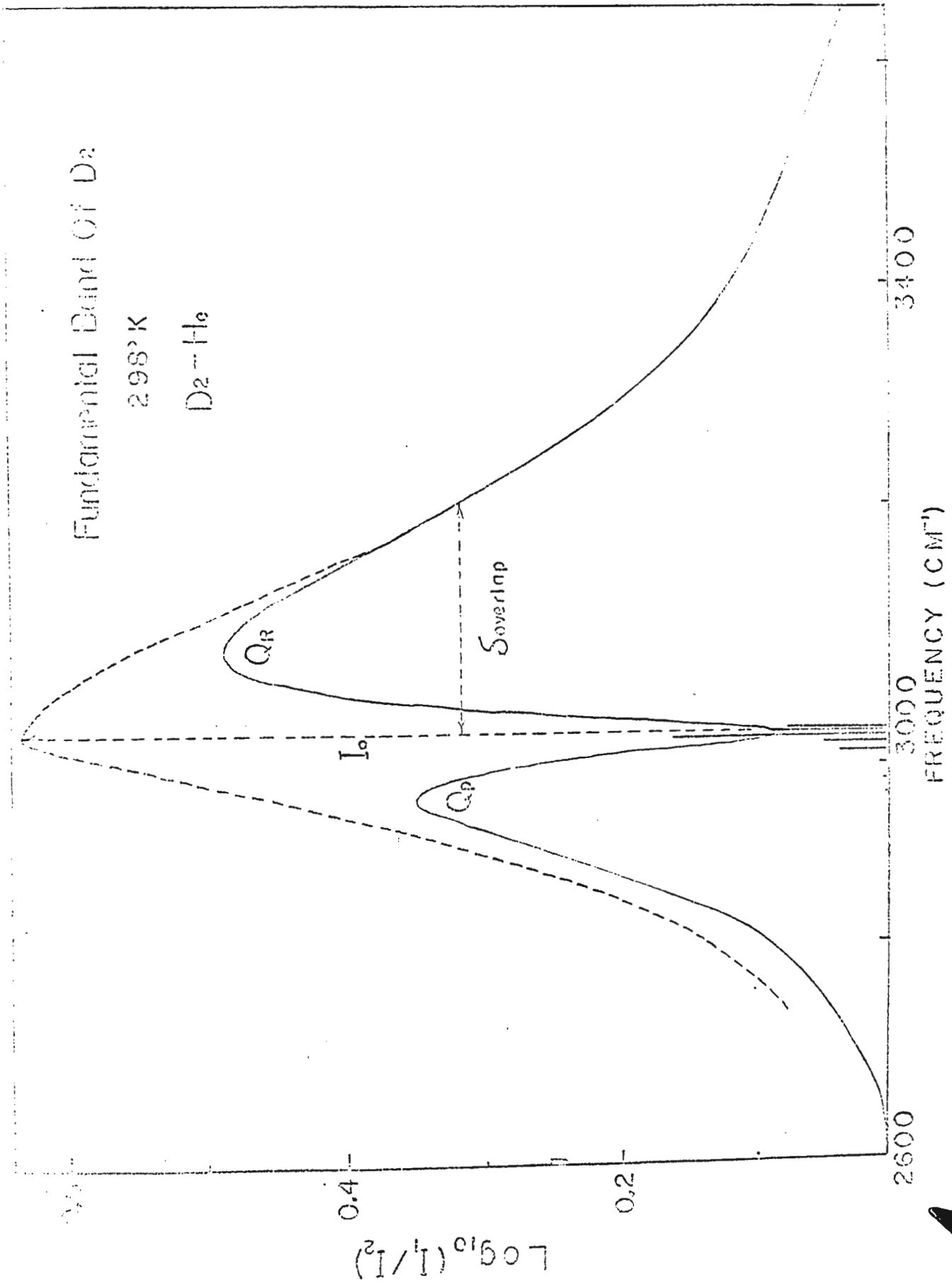
*Values for the pure deuterium contours were obtained from the results of Reddy and Cho (1965)

hydrogen-helium mixtures, Chisholm and Welsh (1954) found that the intensity of the low frequency wing of the Q_p branch, I_- , was related to I_+ by the equation,

$$(25) \quad I_- = I_+ \exp (- \Delta \nu hc/kT),$$

where k is the Boltzmann constant, h is the Plank's constant, c is the velocity of light, and T is the temperature in $^{\circ}K$. An attempt was made to check whether relation (25) is valid for the present band, and an example is shown in Fig. 11. In the figure the dispersion curve obtained for the Q_R branch was used to construct the low frequency wing of the Q_p branch, and the calculated curve is indicated by broken curve. As can be seen in Figure 11, the low frequency wing of the Q_p branch does not agree well with the calculated curve. This discrepancy is probably due to the existence of several lines in the Q branch which are superimposed to give the resultant Q branch in the present contour. All the possible Q lines are shown in the same figure for reference; the vertical line opposite to each Q line is drawn in such a way that its length is proportional to the relative intensity of the corresponding 'overlap' Q line which was calculated from the theory outlined in Chapter IV. In order to verify the above supposition, a test was made as follows: each Q line was broadened to give dispersion line shape for its higher frequency wing and modified dispersion curve by the Boltzmann factor for its low frequency wing, and all the possible broadened Q lines

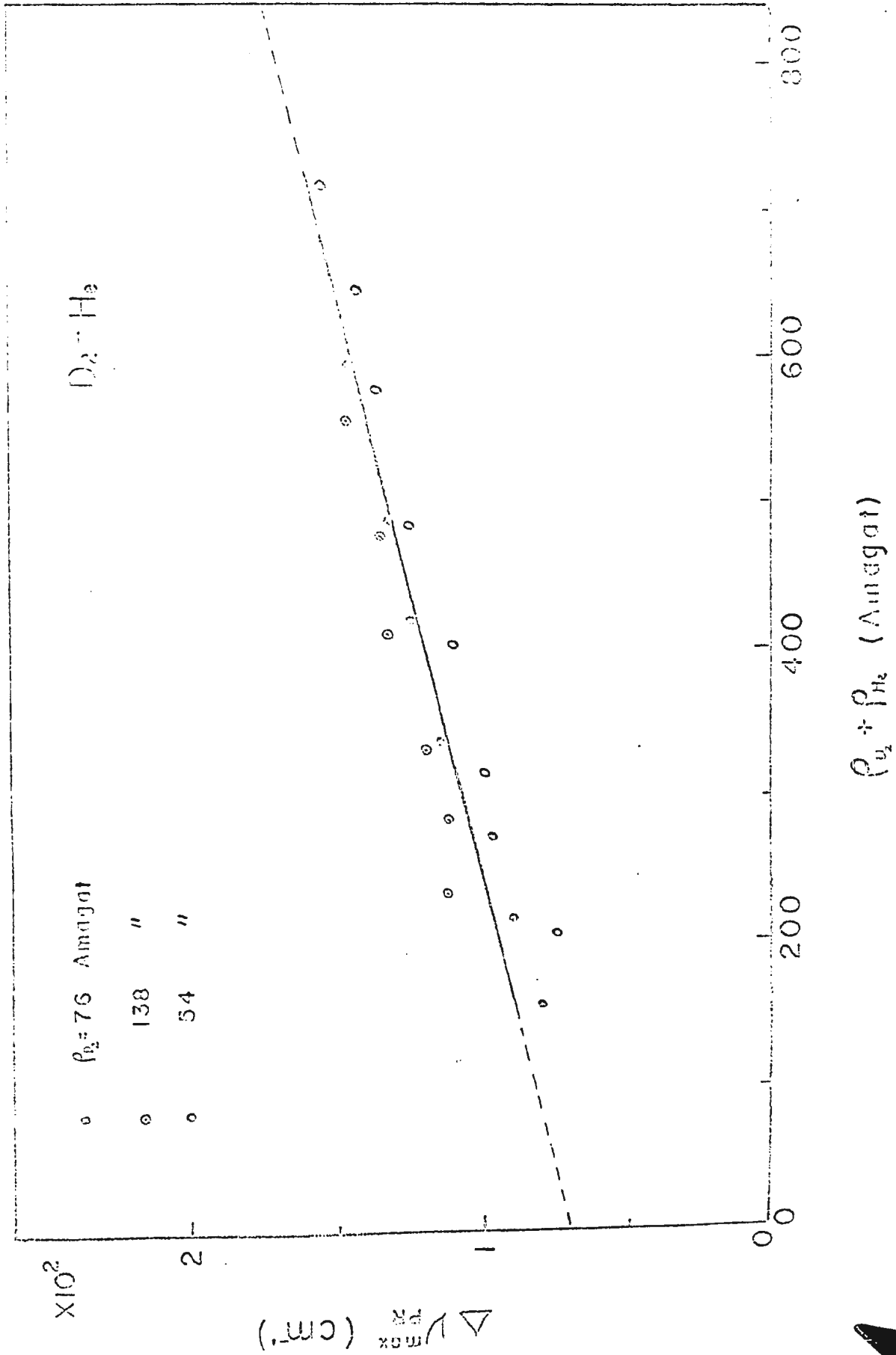
Fig. 11 Profile of the observed absorption contour of the fundamental band of D₂ in a D₂-He mixture.



are added. When the total Q branch thus constructed was examined, the shape of its low frequency wing differed slightly from that of the curve constructed from its high frequency wing using equation (25). However its high frequency wing maintains more or less the same shape represented by equation (24). Thus the present supposition was proved to be correct at least qualitatively.

As has been mentioned in Chapter III, the separation between the Q_P and Q_R peaks was found to increase with the density of the mixtures. Following the method proposed by Hare and Welsh (1958) for the fundamental band of hydrogen, the separation between the Q_P and Q_R peaks, $\Delta\nu_{PR}^{\max}$, for deuterium-helium mixtures is plotted against the total density of the mixture, $\rho_a + \rho_b$, in Fig. 12. As is seen in the figure the plot represents more or less a straight line and the intercept, $\Delta\nu_{PR}^{\max}$ at $\rho_{D_2} + \rho_{He} = 0$, is found to be approximately 70 cm^{-1} . It is interesting to note that this value is almost identical to the corresponding value for the hydrogen band which was given by Hare and Welsh (1958) to be 71 cm^{-1} . This limiting value of the separation may be interpreted as follows: At the moment of the closest approach of the colliding pair of molecules, when the transition probability arising from the overlap interaction is greatest, the colliding pair may be considered a complex resembling a diatomic molecule with its rotational angular momentum quantized. Based on the above consideration the splitting

Fig. 12 The separation between the Q_p and Q_R peaks in D_2 -He mixtures as a function of the total density.



of the Q branch may be considered as a Bjerrum double band arising from such molecular complex. Consequently the limiting value of the separation of the Q_P and Q_R peaks can be used to estimate an average distance of the closest approach between the colliding pair from the equation,

$$(26) \quad \Delta \nu_{PR}^{\max} = (8BkT/hc)^{1/2},$$

where $B = h/8\pi cm \gamma_0^2$, m being the reduced mass of colliding pair and γ_0 the average distance of the closest approach. Result of this calculation is given in Table VIII.

The Absorption Profiles of $D_2 - A$ and $D_2 - N_2$ Mixtures

As was discussed in the beginning of this Chapter the absorption profiles obtained in deuterium-argon and deuterium-nitrogen mixtures presented certain difficulties from the study of each branch of the fundamental band. It was therefore necessary to make certain theoretical assumptions for the purpose of the decomposition of these contours. For the decomposition of the contours, two basic assumptions were made: first, the contours were considered to solely arise from the binary collisions neglecting the effects of ternary collisions, so that the absorption intensities of the individual lines in the band may be calculated directly from the theory outlined in the previous chapter; secondly, each line arising from the quadrupole interactions was assumed to have the shape which

Table VIII

Result of $\Delta\nu_{PR}^{\max}$ and r_0

Perturbing gas	$\Delta\nu_{PR}^{\max}$ at $\rho_a + \rho_b = 0$ (cm^{-1})	r_0 (\AA)	σ^* (\AA)
He	70 (71)	3.0	2.74
A	20 (26)	7.9	3.17
N_2	51 (43)	3.2	3.31

*See the footnote of Table IV.

has been found for the pure rotational lines of hydrogen, i.e., the line shapes given by equations (24) and (25) were assumed to be valid for all the quadrupole lines. The procedure of the decomposition of the band in the present investigation will be presented step by step as follows:

(a) Determination of the O, S and Q_{quad} branches for each observed contour.

- i) Applying the theory proposed by Van Kranendonk, the binary absorption coefficients for all the individual lines of the band are computed, as presented in Chapter IV.
- ii) The percentage fraction of the binary absorption coefficient due to the quadrupole interaction is obtained.
- iii) Choosing a suitable dispersion half-width, each quadrupole line was broadened using the equations (24) and (25).
- iv) Relative total intensity due to the quadrupole lines at a given frequency is computed by adding the contributions from all the quadrupole lines at that frequency and by multiplying the sum by the frequency.

- v) The calculated absorption due to the quadrupole part over the entire band for a particular observed band was normalized using the factor obtained in ii) above.
- (b) Construction of the Q_{overlap} branch for each observed contour was carried out by subtracting the calculated quadrupole branches from the observed contour.
- (c) By the method of trial and error, the most suitable dispersion half-width for quadrupole lines was obtained keeping in view the smoothness of the constructed Q_{overlap} branch.

Using the above method the dispersion half-width of the quadrupole lines, δ_{quad} , could be determined within accuracy of $\pm 10 \text{ cm}^{-1}$. The results are given in Table VII. In Fig. 13, an example of such decomposition is presented. As is seen in the figure the computed total absorption profile agrees well with the experimental contour. In the above procedure of decomposition necessary computations were carried out using the IBM 1620 computer of the Mathematics Department, Memorial University of Newfoundland. The computer program is presented in Appendix.

In Fig. 14 and 15, representative sets of decomposed Q_{overlap} branches for deuterium-argon and deuterium-nitrogen, respectively, are shown. From these Q_{overlap} branches, the dispersion half-widths,

Fig. 13 Decomposition of the fundamental band of D₂ in a D₂-N₂ mixture.

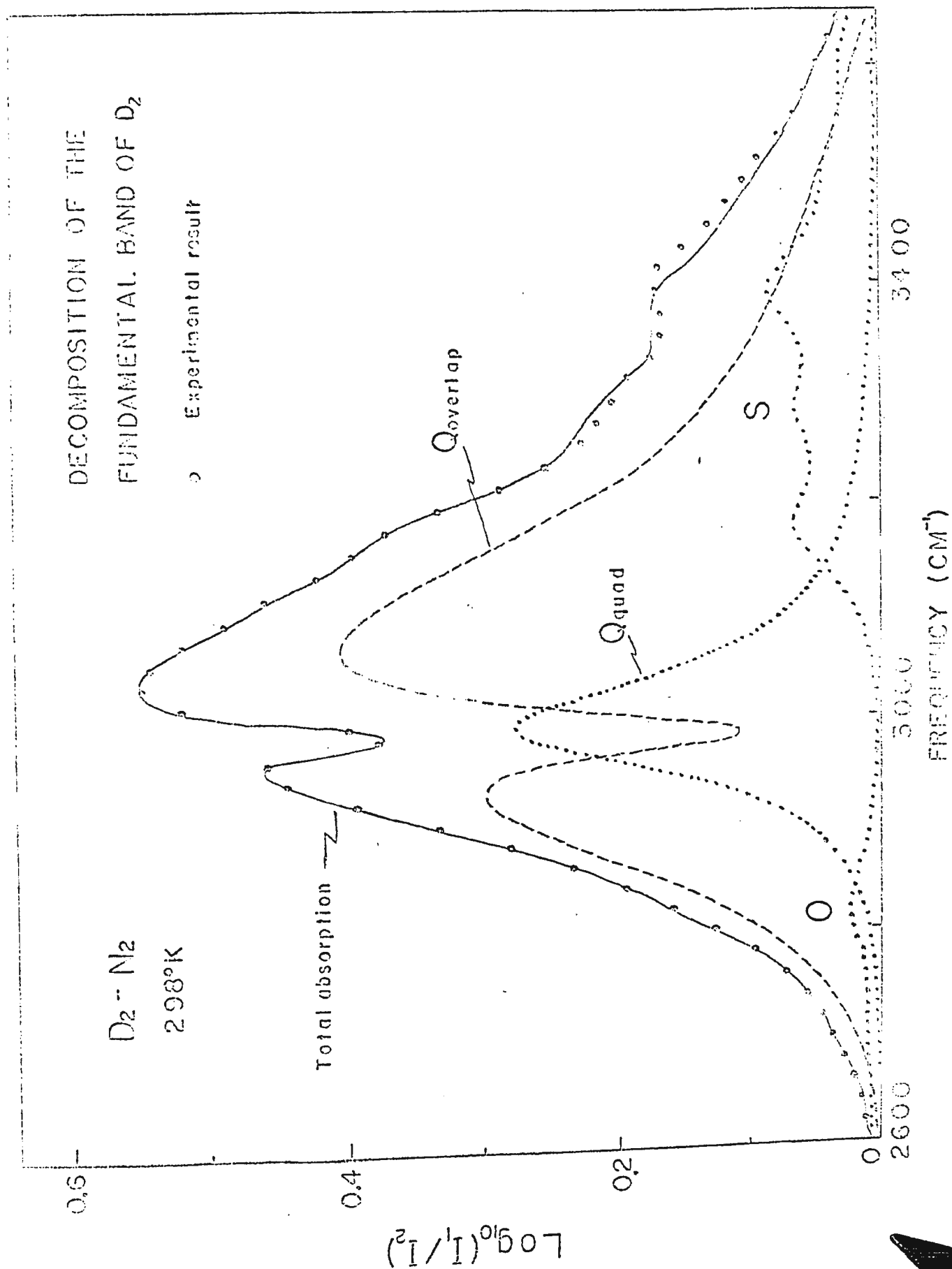


Fig. 14 The overlap part of the Q branch in the fundamental band of D₂ in D₂-A mixtures with a constant base density of D₂.

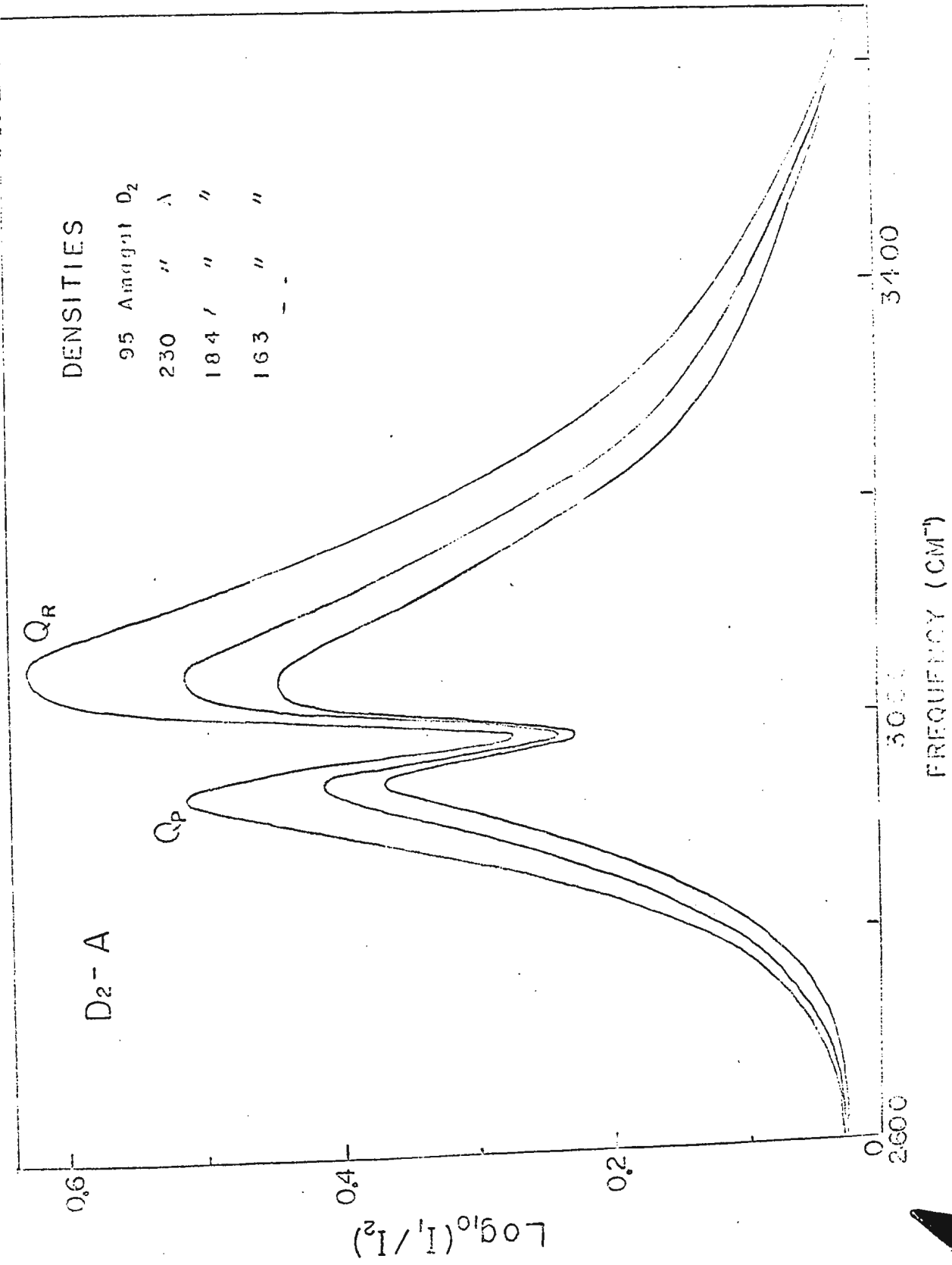
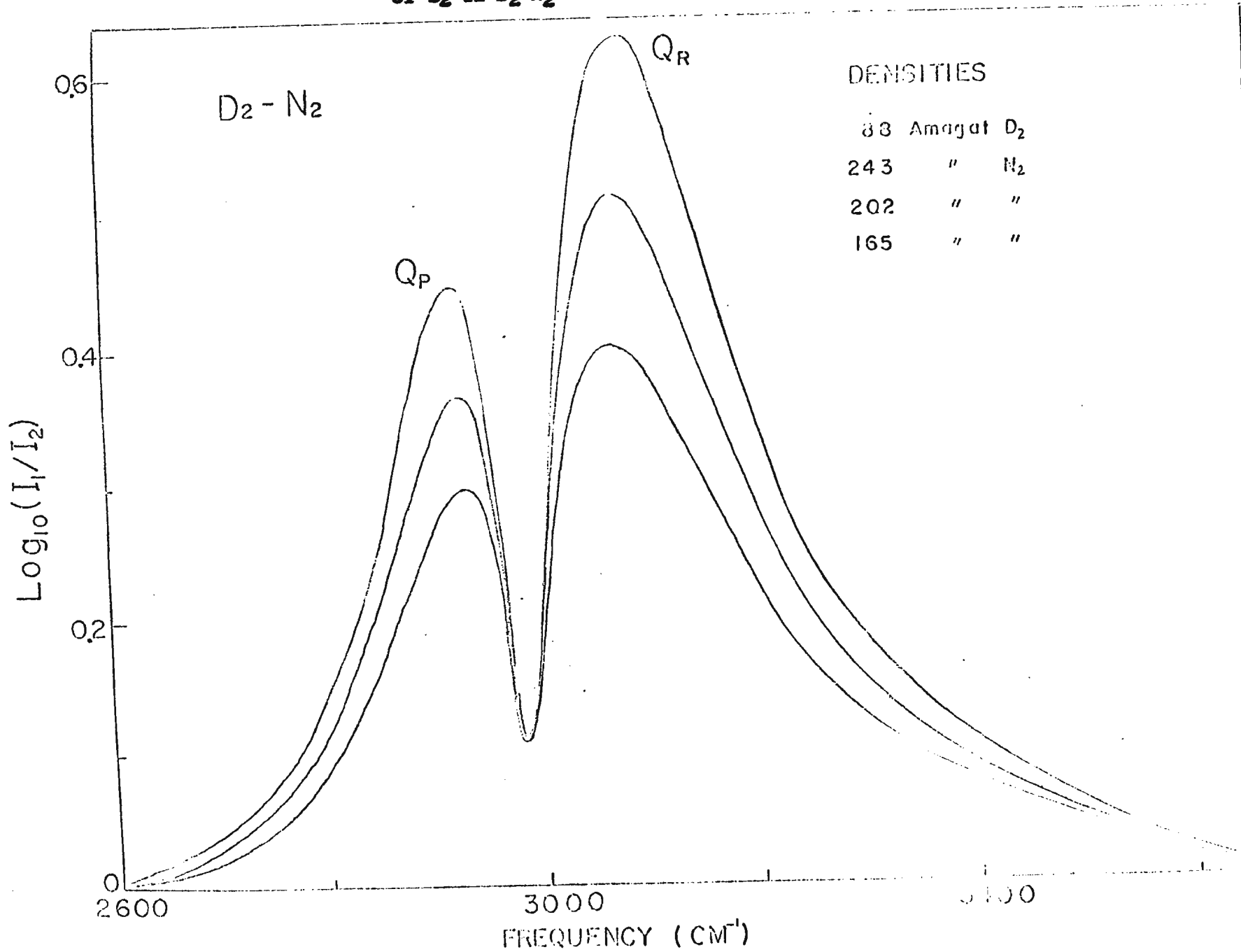


Fig. 15 The overlap part of the Q branch in the fundamental band of ν_2 in D_2-N_2 mixtures with a constant base density of D_2 .



δ_{overlap} , were computed for deuterium-argon and deuterium-nitrogen binary mixtures, following the same method described in the case of deuterium-helium mixtures. The results are given in Table VII. In this table corresponding values for the hydrogen fundamental band obtained by Hunt and Welsh (1964) are presented for comparison. The pure deuterium data which were obtained preliminarily from the observed contours by Reddy and Cho (1965) are also presented. It is interesting to note that the values of δ_{overlap} for the deuterium band do not vary greatly from the corresponding values of hydrogen, while δ_{quad} for deuterium-argon and deuterium-nitrogen mixtures are approximately half of those observed in the hydrogen experiments. The separation between the Q_P and Q_R branches were also obtained from the curves presented in Fig. 14 and 15, and the limiting values are given in Table VIII. These limiting values for the above two mixtures are not so reliable as for the deuterium-helium mixtures, since they are based on rather limited data. However, γ_0 for those mixtures were computed and presented in Table VIII. In the table corresponding values for hydrogen band obtained by Hare and Welsh (1958) are indicated in brackets. It can be seen that the values of $\Delta \nu_{PR}^{\text{max}}$ for deuterium band compare well with those for hydrogen band; and that the values of γ_0 obtained from this investigation agree well with the calculated values except for deuterium-argon mixtures.

As shown above the success of the decomposition method outlined in the present section indicates that the theory proposed by Van Kranendonk is in good agreement with the results obtained in the present investigation.

ACKNOWLEDGMENTS

The research described in this thesis was supervised by Professor C. W. Cho to whom the author is greatly indebted for guidance and assistance during the experimental work and in the preparation of this thesis.

The author is also indebted to Professor S. P. Reddy for his guidance and assistance for the research, and to Professor S. W. Breckon for his encouragement during the research work.

The financial assistance in the form of a Graduate Fellowship, awarded during the academic years of 1963 - 1965 was gratefully received from Memorial University of Newfoundland.

The use of the computer facilities of the Mathematics Department of Memorial University of Newfoundland for the calculations is gratefully acknowledged.

Thanks are also due to Mr. A. J. Walsh and Mr. H. W. Barnes for their assistance in preparing some of the diagrams used in this thesis.

APPENDIX

Source Program for IBM 1620 Computer in Fortran Format

Used for the contour analysis of the fundamental band of
D₂ in D₂ foreign gas mixtures.

```
C CALCULATED INDUCED FUNDAMENTAL BAND OF D2-FORN GAS
C OG=ORIGIN, QMD=DER QUAD MOM, PTD=DER POL'ITY, SLD=LAMDA**2
C WTM=MOL WT, WS=STAT WT SYM LEV, WA=STAT WT ANTISYM LEV
C PROG SW 2 ON FOR INDIVIDUAL LINES
C SW1 ON=WITH NORM SW3 ON= QUAD PART ONLY
C SW4 ON CAL FOR AREA
DIMENSION DEL(3), P(8), FREQ(3,8), ABTN(3,8), TOT(3)
DIMENSION ABQ(8), ABQ1(8), ABO(8), SJ(3)
READ 103
READ 100, BE, ALF, OG, GMD, PTD, WTM, WS, WA
READ 101, EK, SIG, QM, PTY, SLD, DI, DJ
READ 102, TEMP, SW, SWQ, SP, WI, N
IF(SENSE SWITCH 1) 1, 2
1 READ 112, FNOR
2 BV=BE-1.5*ALF
  BO=BE-0.5*ALF
  TK=.6952*TEMP
  DEL(1)=SW/2.
  DEL(2)=SWQ/2.
  DEL(3)=SW/2.
  GM1=3.14159*((4.8E-10)**2)*(SIG**3)*(1.0E-24)/(3.*OG*WTM)
  GMA=GM1/(1835.*(9.1085E-28)*(3.0E+10))
  Q1=QMD*PTY/((SIG/0.529)**4)
  Q2=QM*PTD/((SIG/0.529)**4)
  DO 10 J=1,8
    AJ=J-1
    FREQ(1,J)=OG+2.*BV-(3.*BV+BO)*AJ+(BV-BO)*AJ**2
    FREQ(2,J)=OG+(BV-BO)*AJ+(BV-BO)*AJ**2
10  FREQ(3,J)=OG+6.*BV+(5.*BV-BO)*AJ+(BV-BO)*AJ**2
    SUM=0.
    DO 20 J=1,7,2
      AJ=J-1
      P(J)=(EXP(-BO*AJ*(AJ+1.)/TK))*WS
      P(J+1)=(EXP(-BO*(AJ+2.)*(AJ+1.)/TK))*WA
20  SUM=SUM+(2.*AJ+1.)*P(J)+(2.*AJ+3.)*P(J+1)
    FAC=1./SUM
    DO 200 L=1,3
      IF (L-2) 21, 22, 21
21  DO 30 J=1,8
      AJ=J-1
      SJ(1)=3.*(AJ-1.)*AJ/(2.*(2.*AJ-1.))
      SJ(3)=3.*(AJ+1.)*(AJ+2.)/(2.*(2.*AJ+3.))
30  ABTN(L,J)=(Q1**2)*DJ*GMA*FAC*P(J)*SJ(L)
      GO TO 200
22  SUM=0.
      DO 40 J=1,8
      AJ=J-1
      SJ(L)=AJ*(AJ+1.)*(2.*AJ+1.)/((2.*AJ-1.)*(2.*AJ+3.))
      ABQ1(J)=SJ(L)*(Q1**2)*DJ*GMA*FAC*P(J)
40  SUM=SUM+SJ(L)*P(J)*FAC
      DO 50 J=1,8
      AJ=J-1
      SJQ0=2.*AJ+1.
      ABQ(J)=ABQ1(J)+SJQ0*(Q2**2)*DJ*GMA*FAC*P(J)
      ABO(J)=SJQ0*SLD*DI*GMA*FAC*P(J)
```

```
50 ABTN(L,J)=ABQ(J)+ABO(J)
200 CONTINUE
   IF (SENSE SWITCH 2) 51, 52
51 PUNCH 111, GMA,Q1,Q2
   PUNCH 103
   PUNCH 104
   DO 60 J=3,8
   JJ=J-1
60 PUNCH 105, JJ, FREQ(1,J), ABTN(1,J)
   DO 70 J=1,8
   JJ=J-1
70 PUNCH 106, JJ, FREQ(2,J), ABO(J), ABQ(J), ABTN(2,J)
   DO 80 J=1,8
   JJ=J-1
80 PUNCH 107, JJ, FREQ(3,J), ABTN(3,J)
52 PUNCH 108, SW, SWQ, TEMP
   PUNCH 109
   AREA=0.
   DO 901 K=1,N
   AK=K+0
   W=WI+AK*SP
   IF (SENSE SWITCH 3 ) 310, 315
310 TOTQ=0.
   DO 300 J=1,8
   Y=ABQ(J)/(((W-FREQ(2,J))/DEL(1))*((W-FREQ(2,J))/DEL(1))+1.)
   IF (W-FREQ(2,J)) 301,301,302
301 TOTQ=TOTQ+Y*W*EXP(-(FREQ(2,J)-W)/TK)
   GO TO 300
302 TOTQ=TOTQ+Y*W
300 CONTINUE
315 DO 90 L=1,3
   TOT(L)=0.
   DO 90 J=1,8
   Y=ABTN(L,J)/(((W-FREQ(L,J))/DEL(L))*((W-FREQ(L,J))/DEL(L))+1.)
   IF (W-FREQ(L,J)) 91, 91, 92
91 TOT(L)=TOT(L)+Y*EXP(-(FREQ(L,J)-W)/TK)*W
   GO TO 90
92 TOT(L)=TOT(L)+Y *W
90 CONTINUE
   IF (SENSE SWITCH 3) 400, 410
400 IF (SENSE SWITCH 1) 401,402
401 TOT(1)=TOT(1)*FNOR
   TOT(2)=TOTQ*FNOR
   TOT(3)=TOT(3)*FNOR
   GO TO 500
402 TOT(2)=TOTQ
   GO TO 500
410 IF (SENSE SWITCH 1) 411,500
411 TOT(1)=TOT(1)*FNOR
   TOT(2)=TOT(2)*FNOR
   TOT(3)=TOT(3)*FNOR
   GO TO 500
500 TOTAL=TOT(1)+TOT(2)+TOT(3)
   IF (SENSE SWITCH 4) 600,501
600 AREA=AREA+TOTAL
   GO TO 901
501 PUNCH 110, W, TOT(1), TOT(2), TOT(3), TOTAL
901 CONTINUE
   PUNCH 113, AREA
100 FORMAT(3XF6.0,4XF6.0,3XF7.0,4XF4.0,4XF4.0,4XF8.0,3XF3.0,3XF3.0)
```

```
101 FORMAT(3XF6.0,4XF6.0,3XF4.0,4XF4.0,4XE7.2,3XF5.0,3XF5.0)
102 FORMAT(4XF5.0,4XF6.0,4XF6.0,3XF4.0,3XF7.0,2XI4)
103 FORMAT(40HBINARY ABSORPTION COEFFICIENTS OF D2-D2 )
104 FORMAT(/ 48HLINE FREQUENCY OVERLAP QUADRUPOLE TOT ASTN)
105 FORMAT(2HQ(, 12, 1H), 2XF8.2, 14XE10.2)
106 FORMAT(2HQ(, 12, 1H), 2XF8.2, 2XE10.2, 2XE10.2, 1XE10.2)
107 FORMAT(2HS(, 12, 1H), 2XF8.2, 14XE10.2)
108 FORMAT(18HBROADENED WITH SW=,F7.1,9H AND SWQ=,F7.1, 6H AT T=,F7.1)
109 FORMAT(19HFREQUENCY O-BRANCH,3X29HQ-BRANCH S-BRANCH TOT INT)
110 FORMAT(F8.2, 2XE10.2, 1XE10.2, 1XE10.2, 1XE10.2)
111 FORMAT( 6HGAMMA=, E12.2, 3X 4HMU1=, E10.2, 3X 4HMU2=, E10.2)
112 FORMAT(21X E9.0)
113 FORMAT(6HAREA =,2XE10.2)
STOP
END
```

REFERENCES

- (1) Allin, E.J., Gush, H.P., Hare, W.F.J., Hunt, J.L., and Welsh, H.L. 1959. *Colloq. Intern. Centre Nat. (Paris), Rech. Sci.* 77, 21.
- (2) Allin, E.J., Hare, W.F.J., et McDonald, R.E., 1955. *Phys. Rev.* 98, 554.
- (3) Briton, F.R. and Crawford, M.F., 1958. *Can. J. Phys.* 36, 741.
- (4) Chisholm, D.A., 1952. Ph.D. Thesis, University of Toronto, Toronto, Ontario.
- (5) Chisholm, D.A. and Welsh, H.L., 1954. *Can. J. Phys.* 32, 291.
- (6) Cho, C.W., Allin, E.J. and Welsh, H.L., 1963. *Can. J. Phys.* 41, 1991.
- (7) Colpa, J.P. and Ketelaar, J.A.A. 1958. *Mol. Phys.* 1, 14.
- (8) de Groot, S.R. and ten Seldam, C.A., 1947. *Physica*, 13, 47.
- (9) Ewing, G.E. and Trajman, S., 1964. *J. Chem. Phys.* 41, 814.
- (10) Gush, H.P., Hare, W.F.J., Allin, E.J. and Welsh, H.L., 1960. *Can. J. Phys.* 38, 176.
- (11) Hare, W.F.J., 1955. Ph.D. Thesis, University of Toronto, Toronto, Ontario.
- (12) Hare, W.F.J., Allin, E.J., et Welsh, H.L., 1955. *Phys. Rev.* 99, 1887.
- (13) Hare, W.F.J. and Welsh, H.L., 1958. *Can. J. Phys.* 36, 88.

- (14) Herzberg, G., 1950. Spectra of Diatomic Molecules, I.
- (15) Hirschfelder, J.O., Curtis, F.C., and Bird, R.B., 1954.
Molecular Theory of gases and liquids (Wiley, New York).
- (16) Hodgman, C.D., 1962. Handbook of Chem and Physics.
- (17) Hunt, J.L. and Welsh, H.L., 1964. Can. J. Phys. 42, 873.
- (18) Ketelaar, J.A.A., Colpa, J.P., and Hooge, F.N., 1955.
J. Chem. Phys. 23, 413.
- (19) Kiss, Z.J., Gush, H.P., and Welsh, H.L., 1959. Can. J.
Phys. 37, 362.
- (20) Kiss, Z.J. and Welsh, H.L., 1959. Can. J. Phys. 37, 1249.
- (21) Michels, A., de Boer, J. and Bijl, A., 1937. Physica, 8, 347.
- (22) Michels, A. and Goudekot, M. 1941. Physica, 8, 353.
- (23) Michels, A., Wijker, H. and Wijker, H. 1949. Physica 15, 627.
- (24) Michels, A. and Wouters, H., 1941. Physica, 8, 923.
- (25) Michels, A., Wouters, H. and de Boer, J. 1934. Physica 1, 587.
- (26) Michels, A., Wouters, H. and de Boer, J. 1936, Physica 3, 585.
- (27) Reddy, S.P. and Cho, C.W., 1965. Can. J. Phys. 43, 793.
- (28) Snook, C. 1962. M.Sc. Thesis, Memorial University of
Newfoundland, St. John's, Newfoundland.
- (29) Steynson, C.M., 1965. M.Sc. Thesis, Memorial University of
Newfoundland, St. John's, Newfoundland.
- (30) Stoineff, B. P., 1957. Can. J. Phys. 35, 730.

- (31) Thompson, H.W., 1961. I.U.P.A.C.
- (32) Van Kranendonk, J., 1957. Physica, 23, 825.
- (33) Van Kranendonk, J., 1958. Physica, 24, 347.
- (34) Van Kranendonk, J. and Bird, R.B., 1951. Physica, 17,
953, 968.
- (35) Van Kranendonk, J. and Kiss, Z.J., 1959. Can. J. Phys.
37, 1187.
- (36) Watanabe, A. and Welsh, H.L., 1964. Phys. Rev. Letter,
13, 810.
- (37) Watanabe, A. and Welsh, H.L., 1965. Can. J. Phys. 43, 818.
- (38) Welsh, H.L., Crawford, M.F., and Locke, J.L., 1949. Phys.
Rev., 76, 580.
- (39) Welsh, H.L., Crawford, M.F., McDonald, R.E., and Chisholm, D.A.,
1951. Phys. Rev., 83, 1264.

September 16, 1965

Detailed Comments on M.Sc. Thesis of Mr. S. T. Pai

- (1) In the Abstract, it is not clear what theory is referred to in 'Using the theory and observed line shape'. I presume that Van Kranendonk's theory is intended.
- (2) Some technical terms and jargon, e.g. 'Q branch' on page 1, might well have a few words of explanation or definition when first used. The definition of Q branch does not come until page 4. In a paper for publication the absence of such definitions may be acceptable, but not in a thesis.
- (3) The explanation of Van Kranendonk's model on page 6 is not clear. There is some confusion between the two interactions causing absorption, particularly in the sentence 'In the first interaction'.
- (4) In the description of the experimental apparatus the meaning of the term 'effective length of the cell' on page 10 is not clear.
- (5) In the description of the experimental technique used in placing the foreign gas in the cell some explanation of why the pulsing technique (page 4) works would have been useful. It is clear that, if the length of tubing between V_2 and V_5 is quite short, there is no advantage in using a pulsed, rather than continuous, introduction of foreign gas.
- (6) On page 29 the statement is made that 'The decrease in molecular polarizability at high densities' is probably very small for H_2 '. No justification or plausible reason is presented to support the assertion.
- (7) It would seem clear that the absorption coefficient α_{2a} (page 30) was not observed because of an insufficient range of deuterium pressures.
- (8) In the Calculations for the Deuterium Foreign Gas Mixtures on page 38, the distinction between the calculations performed by Mr. Pai and those obtained from Van Kranendonk's work is not clearly made.
- (9) In Chapter V no mention is made of the effect of the instrumental resolving power. It happens to be very small but this should have been stated.

Comments on Mr. Pai's Thesis, cont'd.

- (10) The statement, on page 51, of the conclusions regarding the shape of the low-frequency wing of the Q_{overlap} curve is not clear. Does the low-frequency wing of the curve constructed by broadening the individual Q components differ slightly from the low-frequency wing of the experimental curve or from the curve constructed by multiplying the high-frequency wing of the experimental curve by the Boltzman factor?. It would have been useful to have all three curves in Fig. 11.
- (11) The computer program listed in the Appendix is extremely difficult to follow as it is presented. Any program of this nature must have a glossary of symbols and a brief description of the program, including the basic formulae that are used.

Errata

Chapter 1

Page 4 line 13 "constant of the"
 line 23 "expect a larger"
Page 5 line 21 "of the induced"

Chapter 2

Page 8 line 6 replace "core" with "bore"
 line 8 the dimension $1 \frac{1}{12}$ in is surely wrong
 "Glyptal"
Page 10 line 1 replace "could" by "would"
 Line 2 "plate"
 line 15 "Unicam"
 line 19 "continuum"
Page 11 line 11 "enhanced"
Page 12 line 12 "The absorption spectrum ..."

Chapter 3

Page 18 line 17,18 Grammatical error: "probably" should precede
 "because"

Chapter 4

Page 35 line 21 " γ_i is the inter - "

Table V

Last line incomplete

Comments

Chapter 2

- Page 10 line 5 I would prefer the words "optical path" in place of "effective"
- line 18 Surely the Globar was operated nearer 200 watts
- Page 11 line 19 Same comments as Page 10, line 5.
- Page 14 line 5,6,7,8 The argument is not quite complete for indeed the gases in the capillary do not mix and therefore, the pure D₂ trace is in error and this error must be reduced.

Chapter 3

- Page 30 line 2,3,4 I consider the argument weak - surely the answer is that $n_a \gg n_b$ in the experiments.

Chapter 4

- Page 30 line 13,14 I think some argument in support of this assumption could be given; I can think of several justifications.
- Page 41 line 1,2 The reference for α' / α should be the original i.e. Terhune and Peters 1959. The value $Q'/ea_0 = .44$ is decidedly not the best. The calculated value of Kolas and Rothaan is undoubtedly better $Q'/ea_0 = .56$. Indeed when the overlap contribution to the rotation lines is included the experiments yield a value much closer to this.

However, I question at this point the assumption that $Q'_{H_2} = Q'_{D_2}$, or even $(Q'/Q)_{H_2} = (Q'/Q)_{D_2}$ as being completely unjustified. This is a very sensitive molecular parameter and may be quite different in the two molecules. This does not prevent one from making the assumption but a word of caution should have been introduced at this point.

Chapter 5

- Page 46 Eqn 24 This equation as applying directly to the results at hand is in error.

Comments - page 2

It should read:

$$\tilde{I}_+ = \tilde{I}_0 / \left\{ 1 + \left(\frac{\Delta\nu}{\delta} \right)^2 \right\} \quad \text{or}$$

$$\text{or} \quad I_+ = I_0 \frac{\nu_+}{\nu_0} / \left\{ 1 + \left(\frac{\Delta\nu}{\delta} \right)^2 \right\}$$

Page 49 Eqn (25) Should be

$$\tilde{I}_- = \tilde{I}_+ \exp(-\Delta\nu h c/kT)$$

see Kiss and Welsh, J.Can. Phys. 37 p 1251 (1959)

lines 11 to 15

This argument is erroneous and unnecessary. It is wrong since the sum of any number of dispersion lines of the same δ and ν_0 (or nearly) is a dispersion line of unaltered δ and ν_0 (or nearly). The bad fit of figure 11 is entirely due to the error in equation (25). If the ordinate at 2800 cm^{-1} is multiplied by the ratio ν_+ / ν_- the error is removed

$.94 \frac{3200}{2800} = 1.23$ which falls exactly on the calculated curve.

